LUT UNIVERSITY
LUT School of Energy Systems
LUT Mechanical Engineering

Riku Peltonen

PROCESS SOLUTIONS OF EXTRUSION-BASED ADDITIVE MANUFACTURING FOR GEOPOLYMERS AND 3D PRINTABLE MATERIAL PROPERTIES

Examiners: Professor Timo Kärki
D.Sc. (Tech.) Anna Keskisaari

TIIVISTELMÄ

LUT-Yliopisto
LUT Energiajärjestelmät
LUT Kone

Riku Peltonen

Prosessi ratkaisut pursotukseen perustuvaan lisäävään valmistukseen geopolymeereille ja 3D-tulostettavan materiaalin ominaisuudet

Diplomityö

2019

106 sivua, 35 kuvaa, 13 taulukkoa ja 2 liitettä

Tarkastajat: Professori Timo Kärki
TkT Anna Keskisaari

Hakusanat: lisäävä valmistus, 3D tulostus, pursotus, kierrätettävät materiaalit, materiaali lujuus, materiaalin käyttäytyminen

Geopolymeerien käyttämisellä rakennusteollisuudessa tavallisten betonien sijasta on potentiaalia vähentää tuotettuja CO_2-päästöjä merkittävästi. 3D-tulostuksen käyttöönotto lisää kestävää kehitystä entisestään, kun jätteeksi päätyviä kertakäyttöisiä muotteja ei tarvita. Tämän työn tavoitteena oli kehittää kestävä geopolymeerimateriaali, jota voidaan käyttää 3D-tulostamiseen, sekä löytää konseptiratkaisu geopolymeeri 3D-tulostimelle. Paperi-kaivos- ja rakennusteollisuuden sivuvirtoja käytettiin geopolymeerin raaka-aineina.

Tutkimus on jaettu kirjallisuuskatsaukseen, geopolymeerimateriaalien kehitykseen ja geopolymeerimateriaalien testaukseen. Kirjallisuutta hyödynnettiin geopolymeerin 3D-tulostuksen erityispiirteiden, laitteistoratkaisujen, sekä geopolymeerimateriaalin kehittämisen suuntaviivojen ja testauksen selvittämiseen. Materiaalin kehitys perustui systemaattiseen lähestymistapaan, jossa kehitettyjä materiaaliyhdisteitä arvioitiin numeerisesti usealla eri osa-alueella soveltuvan datan mukaisesti. Tuoreen materiaalin ominaisuuksia tutkittiin kovettumisaika- ja muodonsäilyvyyskokeilla. Standartoituja menetelmiä käytettiin kovettuneen materiaalin puristus- ja taivutuslujuuksien kokeissa.

Parhaiten 3D-tulostukseen kehitetyissä ja soveltuvissa geopolymeereissä oli 56–58% kierrätettyjä materiaaleja. Lämmityksen havaittiin parantavan huomattavasti materiaalin kerrostettavuutta ja kovettumisaikaa. Reagoivien kierrätysmateriaalien kokonaismäärän ollessa yli 20%, materiaalin lujuus ja työstettävyys heikkenivät. 7 ja 28 päivän kovettumisajan välillä lujuudet kasvoivat puristuksessa ja heikkenivät taivutuksessa. Kerrostetut koekappaleet olivat lujuudeltaan heikompia puristuksessa ja vahvempia taivutuksessa. Parhaimpien koekappaleiden lujuudet olivat 13–45% heikompia kuin pienimmät lujuusarvot 3D-tulostettavilla geopolymeereillä yleensä. Geopolymeerin kehityksen havaittiin olevan kompromissien tekoa eri lujuuksien ja kierrätettävien materiaalien määrän välillä. 3D-tulostetuilla geopolymeereillä voi kilpailla rajoitetusti perinteisen valmistuksen kanssa keskittymällä erikoistuneisiin ja monimutkaisiin tuotteisiin.

ABSTRACT

LUT University
LUT School of Energy Systems
LUT Mechanical Engineering

Riku Peltonen

Process solutions of extrusion-based additive manufacturing for geopolymers and 3D printable material properties

Master's thesis

2019

106 pages, 35 figures, 13 tables and 2 appendices

Examiners: Professor Timo Kärki
D.Sc. (Tech.) Anna Keskisaari

Keywords: additive manufacturing, 3D printing, extrusion, recyclable materials, material strength, material behavior

Use of geopolymers in construction industry instead of traditional concretes has the potential to reduce produced CO_2 emissions significantly. 3D printing can be utilized to promote sustainability even more as disposable formwork is not required that generate waste. The aim and goal of this study were to develop sustainable geopolymer material applicable in 3D printing and to find a concept solution for a geopolymer 3D printer. Side streams of paper, mining and construction industries were used as geopolymer raw materials.

The research was divided between the literature review, geopolymer material development, and geopolymer material testing. Literature was used to determine the peculiarities of 3D printing geopolymers and to find existing 3D printer solutions and guidelines for geopolymer material development and testing. Material development was based on a systematic approach by evaluating generated material mixtures with numerical values in multiple steps based on existing data. Fresh material behavior of geopolymer was examined with setting time and shape stability tests. Standardized test methods were utilized in the testing of hardened material properties of compressive and flexural strengths.

Most suitable developed 3D printable geopolymers had 56–58% recycled material content. Heating was found to improve buildability and setting of material significantly. Higher than 20% reactive recyclable material content caused strength and material workability to decrease. Between 7 and 28 days of curing compressive strength increase while flexural strength was observed to decrease. Layers in test samples caused strength to decrease in compressive and increase in flexural strength test. Highest strength values of test samples were 13–45% lower than the lowest strengths in 3D printable geopolymers in general. Geopolymer development was found out to be a compromise between different strength values and recyclable material content. 3D printing of geopolymers can compete in limited markets with traditional manufacturing by focusing on specialized and complex shape products.

ACKNOWLEDGEMENTS

First, I would like to express my gratitude to Timo Kärki for providing me this interesting topic. I would also thank for all the invaluable guidance and advice throughout this thesis.

Special thanks to Anna Keskisaari for all the great suggestions and continuous feedback. She has spent countless hours of her valuable time in the laboratory to help me conducting the experiments in time.

I would also like to thank everyone who has supported me during my years of studying. Also, thanks to everyone who has been involved even slightly in the making of this thesis from the staff of Fiber Composite Laboratory and university.

Last but not least, I would like to thank my whole family for supporting me through my life and during my studies.

Riku Peltonen
Lappeenranta 9.4.2019

TABLE OF CONTENTS

LIST OF ABBREVIATIONS

3D	Three dimensional
AM	Additive Manufacturing
CC	Contour Crafting
CDW	Construction and Demolition Waste
FDM	Fused Deposition Modeling
GGBS	Ground Granulated Blast Furnace Slag
LoI	Loss on Ignition
OPC	Ordinary Portland cement

1 INTRODUCTION

Additive manufacturing (AM) is a term used for processes that makes objects from data of 3D (three dimensional) models by joining materials typically layer upon layer. Opposite to AM are subtractive and formative manufacturing methods where material removing or shaping is needed for creating the final part. There are several methods in AM for the part manufacturing. Material extrusion is defined as a process where a nozzle or an orifice is utilized to dispense material selectively according to 3D model data. (SFS-EN ISO/ASTM 52900 2017) AM is also known as 3D printing and those abbreviations are used as synonyms even though 3D printing has been commonly used to describe prototyping. 3D printing is currently used for any process that utilizes additive methods without considering the technology, application or material to be printed. (Labonnote et al. 2016) Both abbreviations AM and 3D printing are used through this study to describe the same process.

Geopolymers are discussed generally as geopolymer cement, concrete and paste materials. Geopolymers have been developed mainly in construction industries to substitute ordinary Portland cement (OPC) as an eco-friendlier solution since by-products of other industries containing amorphously Si and Al can be utilized in the geopolymer formulation. (Ma et al. 2018a, Panda & Tan 2018) Polymerizing aluminosilicate materials by activating them with an alkaline solution creates geopolymer materials (Ma et al. 2018a).

A growing population creates a need for sustainable housing, buildings and other infrastructural elements that are commonly made from concrete. AM in the construction industry is mostly relying on extrusion 3D printing processes. More complex freeform objects can be made with 3D printing compared to traditional methods, which need the use of formwork. (Panda & Tan 2018) Since the construction industry has been using concrete made from OPC, the 3D printing developments for construction and infra printing has adopted the same or similar materials. Use of geopolymers for the same purpose has followed in order to make construction and infra building more sustainable. (Panda et al. 2017b)

Main areas involved in this research are extrusion-based additive manufacturing, the behavior of printable cementitious materials and material mechanical properties testing which creates the framework for this thesis as illustrated in Figure 1.

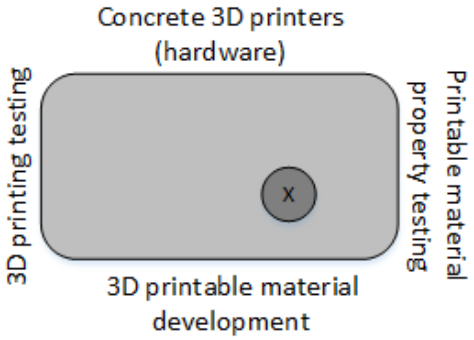

Figure 1. The framework of the study. Focus between the four main areas is marked with the circle and x.

More precisely extrusion-based AM goes into the machine structure framework of the printers (pumps, nozzles, mixers). 3D printable geopolymer material development and material property testing are on the main focus.

1.1 Motivation for 3D printing of geopolymers

AM is adapted to many different industries in a more increasing rate. Construction and other building industries that use concrete or cementitious materials are not exceptions. The traditional building of concrete materials requires formwork for the object to be made. Formwork is time-consuming and requires skilled labor. (Panda et al. 2017b) Up to 30% of materials used in traditional techniques of working with concrete goes to waste (Ghaffar et al. 2018). Use of molds can limit the shape of the object to be manufactured due to cost and physical limitations. With the use of AM, the need for an extensive formwork can be eliminated and most of the labor force can be reduced. Distribution of a typical concrete construction project cost is shown in Figure 2.

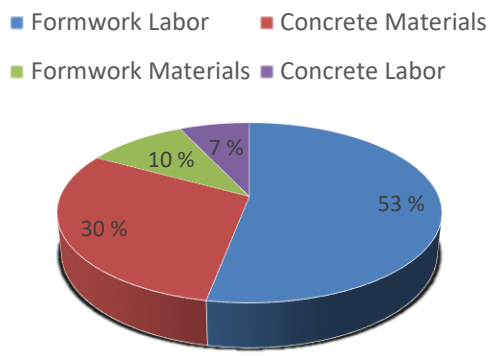

Figure 2. Average cost distribution of concrete construction projects (Mod. Paul et al. 2018a).

It can be clearly seen in Figure 2 how the formwork takes a significant amount of total costs. Total time for the formwork from a total construction time is usually between 50–75% (Paul et al. 2018b). Applying AM in the applications where concrete is utilized with traditional techniques will offer reduced CO_2 (carbon dioxide) emissions when the entire product life cycle is considered, since the material use and waste can be lowered with the elimination of formwork (Ghaffar et al. 2018, Paul et al. 2018b).

Even though AM can lower CO_2 emissions, the issue with using OPC alone and as a binder in concrete is that the production of the cement materials produces large amounts of CO_2 emissions (Kashani & Ngo 2018). Use of concrete (and OPC as a binder) is vast around the globe being the most used construction material and only water is consumed more by communities. The production of 1 tonne of OPC generates 0,95 tons of CO_2 mainly due to calcination of calcium carbonate which is not required in the manufacturing of geopolymer cement. Reduction of CO_2 emissions in geopolymer cement production compared to OPC is in range of 40% to 80–90% depending on the type of geopolymer cement. Furthermore, energy need in production can be 43–59% lower for geopolymer cement. (Davidovits 2013)

3D printable geopolymers have the potential to be an environment-friendly alternative for the OPC based counterparts as geopolymers can reduce CO_2 emissions and climate change respectively (Panda et al. 2017b). Studies on geopolymer-based materials (pastes, cements and concretes) for use in AM applications have been emerging in recent years by several authors. The focus of the studies is mainly material development and testing of fresh and

hardened material properties. Geopolymer materials and 3D printing systems suitable for geopolymer printing are still vastly under development, for example in studies of Panda et al. (2018a), Paul et al. (2018a), Nematollahi et al. (2018) and Ma et al. (2019).

1.2 Research problem

Concrete can be 3D printed with several different configurations which are also suitable for printing of geopolymers. How to choose the optimal configuration to a specific purpose remains unclear. AM of geopolymer materials with material extrusion process is highly dependent on the material mixture and parameters used during the extrusion. It is unclear how to choose printing parameters for newly developed materials to achieve suitable printing quality and maximized mechanical properties.

There are no guidelines for geopolymer material development and testing for 3D printing purposes. How different contents of aluminosilicate materials affect on the fresh and hardened material properties is unclear. Testing of the fresh and hardened 3D printable geopolymer material properties have been carried out with several different test methods, yet there is no agreement on the methods that should be utilized to test specific material printing and hardening properties.

It is recognized that geopolymer reacts to heat and it can introduce better mechanical properties and faster strength development. Applying heat directly to extruded geopolymer in 3D printing process has not been studied or discussed and its effect on the behavior of geopolymer under printing is unclear.

1.3 Objectives

The main objective is to study and research the 3D printing process and equipment of geopolymers and develop 3D printable geopolymer material utilizing locally sourced raw materials. Mixers, pumps and nozzle solutions are studied and their characteristics and suitability for 3D printing applications are presented and evaluated. Concept idea of geopolymer 3D printer will be constructed based on existing 3D printing machine solutions and properties of developed material for certain capacity. Studies on 3D printing of geopolymer and other cementitious and concrete-like materials are investigated, and their compositions are studied in order to find guidelines for material development. Testing

methods of 3D printable geopolymer material properties in the fresh and hardened state are evaluated to find suitable testing methods for the material under development.

Objectives in practical part are to develop and test the extrusion, proper mixing time, open time and structural properties of the newly developed geopolymer. To test fresh properties of the newly developed geopolymer mix and to find proper combination for successful 3D printing of part, component or structure. Hardened properties of the printed samples are investigated to find combination for further printing projects.

1.3.1 Research questions

There are plenty of unclear areas related in geopolymer based 3D printing as described in the research problem. In this study the following main research questions derived from the research problem are answered:

- What kind of machine setups are suitable for 3D printing of geopolymer?
- What are suitable mixing rates of aluminosilicate containing waste materials in order to attain 3D printable geopolymer?
- How do different heating temperatures affect setting time, buildability, workability and strength properties of 3D printable geopolymer?
- How do different waste materials and layering parameters affect on 3D printable geopolymer strength properties?

1.4 Research methods

Research is divided into three parts: literature review, material development and material testing. A literature review was conducted by systematically searching publications related to 3D printing of geopolymers. From the literature answers where obtained for some of the research questions and information was collected about testing methods and procedures that were used as a base for laboratory tests in material testing and printing simulations. Databases that were utilized in the research were mainly Scopus, ScienceDirect, SpringerLink and Emerald Insight. Search was done by using a list of keywords and creating search string using Boolean operators and dividing search words by action of “how” and “what”. Relevant studies where screened from the search results with following qualitative criterion which studies had to be related:

- Extrusion-based 3D printing of geopolymers, concrete-like and cementitious materials
- Processing of geopolymers, concrete-like and cementitious materials
- Geopolymer preparation and testing

Results of the literature review are presented in following chapters and they were used as a basis for the actual physical geopolymer material development and printable material property tests by examining the methods that were applied in other studies of 3D printable geopolymers. Standard methodologies and procedures were implemented to research in parts where they were evaluated to be suitable.

1.5 Scope

Geopolymers have a wide range of applications and definitions. The scope is on geopolymer cements, concretes, mortars and pastes which have been described in the literature of 3D printing of geopolymers. Due to similarities in AM systems in concrete and geopolymer printing equipment that have been only tested for concrete are also included. The main focus is in on nozzle and printing head, mixing and pumping that are dependent on the printable material. Other areas of printer equipment structures are not described in detail.

Practical arrangements are planned for testing of two geopolymers that are formulated from locally sourced ingredients and waste materials that contain aluminum and silicon. The tests are focused on testing the setting time, buildability and mechanical properties by flexural and compression testing. The effect of heat in the setting time and buildability properties are the main interest. Fresh material properties testing in this study focuses on the properties that material has straight after extrusion to the point it has hardened beyond extrudability. Material behavior is studied in 3D printing point of view. End use for the geopolymer is set to be in 3D printing of structural wall elements. Chemical and geopolymerization process of material is not on the scope.

2 GEOPOLYMERS

The high cost of production has kept the geopolymers away from large scale constructions and other implementations even though research on the geopolymer materials has been continued from the 1950s to this day. Geopolymers can have a niche application area where specific properties are needed for mechanical, chemical or fire resistance. (Kolezynski et al. 2018) Geopolymers for creating cement and concrete are generally introduced and the main focus is kept on 3D printing applications.

2.1 Geopolymers in general

Geopolymers are usually used as a binder to form a material that has similar properties and composition as concrete. Geopolymers are aluminosilicate-based materials and their durability, thermal and mechanical properties can be good as or better than in traditional concrete made with OPC, depending on the chemical composition of ingredients. Common precursors used in geopolymers are fly ash, blast furnace slag and silica fume or metakaolin. (Kashani & Ngo 2018, Panda et al. 2018a) Disadvantages for geopolymers are generally faster setting time, higher shrinkage than in OPC and the need for curing in above room temperatures (Panda et al. 2018a). Simplified reaction mechanism for geopolymerization is illustrated in Figure 3.

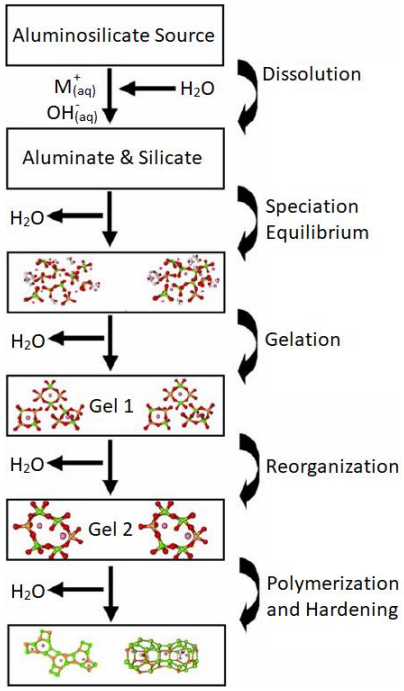

Figure 3. Geopolymerization process (Mod. Duxson et al. 2007).

In the first stage of geopolymerization process, the solid aluminosilicate sources dissolve in alkaline hydrolysis into aluminate and silicate species. Chemical equilibrium is then achieved, and supersaturated aluminosilicate is formed. Supersaturated aluminosilicate solution turns into a continuous gel in time that varies depending on system conditions and some systems never gel. (Duxson et al. 2007) Rearrangement and reorganization starts, and connectivity in the gel network increases which results in 3D aluminosilicate network (Si–O–Al–O bonds) (Duxson et al. 2007, Ma et al 2018a). Last hardening stage may vary vastly from hours to weeks depending on the raw materials and other variables in the system. The geopolymerization process described above is simplified and each step has exceptions and their own field of studies. No particular geopolymerization process can be presented that would satisfy all geopolymers since the process is case sensitive. (Duxson et al. 2007)

Geopolymers are called more precisely as geopolymer cement when there are no stone aggregates added to the mixture. After adding of aggregates to the geopolymer cement, the mixture is called geopolymer concrete which is classified as a composite material. Rock-based aggregates are suitable for geopolymer cements and they can form strong chemical bonds. Alkaline reagents used to create the geopolymer are usually sodium or potassium soluble silicates with the addition of water. The molar ratio of the silicates should be

SiO_2:M_2O>1,65, where M is either sodium or potassium. Geopolymer cements are rapidly curing within 24 hours and they harden in room temperatures with the addition of calcium cations. (Davidovits 2013)

Alkaline reagents used in the geopolymer cements can be classified as corrosive (hostile) and irritant (friendly). Corrosive products for geopolymer cements cannot be easily implemented on a large scale because of safety regulations and laws. Handling of corrosive products requires the use of masks, gloves and glasses as safety equipment. (Davidovits 2013) In Table 1 hostile and user-friendly alkaline-reagents are presented.

Table 1. Classification of alkaline reagents (Davidovits 2013).

Hostile	Friendly
CaO (quick lime), NaOH, KOH	$Ca(OH)_2$, Portland cement, Iron slag
Sodium metasilicate SiO_2:Na_2O = 1,0	Slurry soluble silicate/kaolin 1,25<SiO_2:Na_2O<1,45
Any soluble silicate SiO_2:Na_2O<1,45	Any soluble silicate SiO_2:Na_2O>1,45

Geopolymer cements can be classified in four following categories according to Davidovits (2013):

- “Slag-based geopolymer cement
- Rock-based geopolymer cement
- Fly ash-based geopolymer cement
    - type 1: alkali-activated fly ash geopolymer
    - type 2: slag/fly ash-based geopolymer cement
- Ferro-sialate-based geopolymer cement”

Slag-based geopolymer cements are a combination of blast furnace slag, metakaolin and user-friendly alkali silicate. Rock-based geopolymer cements are similar to the slag-based counter ones with the exception of added volcanic tuff to replace metakaolin in a certain amount. Fly ash geopolymer of type 1 is not made as cement instead, it is prepared straight

as concrete. Type 1 fly ash uses sodium hydroxide that is hostile to users and the resulting concrete usually needs heat hardening. Fly ash geopolymer cement of type 2 is made from user-friendly silicate solution, fly ash and blast furnace slag. Ferro-sialite-based geopolymer cements have high iron oxide content elements added to them and are otherwise close to rock-based geopolymers. (Davidovits 2013)

2.2 Geopolymers for extrusion AM

With the common precursors for geopolymers and activators, there are countless possibilities for different mixture designs. (Kashani & Ngo 2018) Information of geopolymer compositions for extrusion AM used in different studies where gathered in order to find out the suitable mixtures. Particularly amounts of Al_2O_3 (aluminum oxide) and SiO_2 (silicon dioxide) used in mixes where under interest. The mentioned chemicals are found in fly ash, ground granulated blast furnace slag (GGBS) and silica fume that are the main ingredients used for creating printable geopolymers (Kashani & Ngo 2018). Some studies have examined the used ingredients with X-ray fluorescence (XRF) where the chemical composition is shown precisely. Many studies still only describe the amounts of the fly ash, slag and silica fume without describing their chemical compositions, for example studies of Paul et al. (2018a) Panda et al. (2017a), Panda et al. (2018a), Lim et al. (2018), Ma et al. (2019). Typical composition of class F fly ash, GGBS and silica fume are presented in Table 2 according to ASTM. Fly ash composition used in studies is commonly reported as a fly ash grade F. According to standard ASTM C618-12a (2012) class F fly ash contains three main compounds as follows: “SiO2 + Al2O3 + Fe2O3 = 89,15 % > 70 % and CaO < 10 %”.

Table 2. Typical composition (weight %) for fly ash class F, GGBS and silica fume (Kosmatka et al. 2002).

Component	Fly ash [%]	GGBS [%]	Silica fume [%]
SiO_2	52	35	90
Al_2O_3	23	12	0,4
Fe_2O_3	11	1	0,4
CaO	5	40	1,6
Others	3,8	2,7	3,1
LoI	2,8	1	3

3D printable geopolymer mixes usually contain sand, different kind of reagents and additives in addition to the fly ash, slag and silica fume seen in compositions used in studies listed in Table 3, which also presents the mixing ratios of the main ingredients in 3D printable geopolymer mixes and the total approximate percentage of SiO_2 and Al_2O_3 from precursors in those mixes, since detailed information was not provided from the material compositions in all of the studies (marked with *). Values from Table 2 were used for the calculation of the percentage of SiO_2 and Al_2O_3 for studies with missing information on compositions. All values presented are rounded to one decimal accuracy.

Table 3. Mixing ratio of ingredients and percentage of SiO2 and Al2O3 in total mass (1: Kashani & Ngo 2018, 2: Nematollahi et al. 2018, 3: Panda et al. 2018b, 4: Panda & Tan 2018, 5: Panda et al. 2017b, 6: Paul et al. 2018a, 7: Panda et al. 2017a, 8: Panda et al. 2018a, 9: Lim et al. 2018, 10: Zhang et al. 2018, 11: Al-Qutaifi et al. 2018, 12: Ma et al. 2019).

Reference	Fly ash	Slag (GGBS)	Silica fume	Sand	Reagents + water	Additives	SiO_2 [%]	Al_2O_3 [%]
1(2	46,8	15,6	7,8		29,8		32,4	13,9
2(2	34,6			51,9	13,1	0,4	17,7	8,8
3	25,7	1,5*	4,6*	54,8	12,9	0,5	17,3	10,3
4(2	27,2	4,9	2,7	48,0	17,2		17,5	11,5
5	27,9	1,7	3,3*	49,6	16,7	0,8	19,9	8,7
6	28,4*	1,7*	3,4*	51,4	14,2	0,9	18,4	6,7
7(2(3	22,9*	4,6*	3,0*	46,7	21,9	0,9	17,4	8,8
8(2	25,3*	5,1*	3,4*	50,7	15,5		18,0	6,4
9(3	27,1*	5,1*	1,6*	51,1	15,2		17,3	6,9
10(2		81,8; 9,1(1			9,1		30,0	12,6
11(2	39,7			39,7	20,6		20,3	10,1
12(2(3	23,9*	9,3*	4,1*	44,8	17,7	0,2	15,7	6,6

1) Steel slag, 2) Most suitable form several tested mixes, 3) Reinforcement fibers as additives

Additives in the geopolymer mixes can be glass or steel fibers or thixotropic additives that gives geopolymer more printable properties. Example of thixotropic additives is magnesium

aluminum silicate nano clay (Lim et al. 2018). Micro steel cables (1,2 mm and 1 mm in diameter) have been also used inside 3D printed geopolymers to increase flexural strength (Ma et al. 2019, Lim et al. 2018).

Alkaline reagents for the geopolymer mixes are liquid activators alone or powder like with the addition of water before or after mixing with the other dry ingredients. Used reagents are for example: sodium meta-silicate powder, potassium silicate and potassium hydroxide. Different activators can be mixed together for required printability (Lim et al. 2018, Panda et al. 2017a, Panda et al. 2017b). List of reagents used in the above studies are presented in Table 4.

Table 4. Alkaline reagents used in geopolymers. (1: Kashani & Ngo 2018, 2: Nematollahi et al. 2018, 3: Panda et al. 2018b, 4: Panda & Tan 2018, 5: Panda et al. 2017b, 6: Paul et al. 2018a, 7: Panda et al. 2017a, 8: Panda et al. 2018a, 9: Lim et al. 2018, 10: Zhang et al. 2018, 11: Al-Qutaifi et al. 2018, 12: Ma et al. 2019).

Alkaline reagent / Reference	1	2	3	4	5	6	7	8	9	10	11	12
Sodium (meta)silicate (Na_2SiO_3)	x	x								x	x	x
Sodium hydroxide (NaOH)		x		x						x	x	
Potassium (meta)silicate (K_2SiO_3)			x	x		x	x		x			
Potassium hydroxide (KOH)					x							
Potassium oxide (K_2O)					x	x						
Hydroxypropyl methylcellulose							x					

In the study of Panda et al. (2018a) used reagent was not described. Properties of geopolymers are governed with the use of alkaline activators with witch the dissolution of silicon and aluminum components from aluminosilicate precursors is accelerated and formation of prepolymers is promoted (Zhang et al. 2018). The molar ratio of the used silicates should be > 1,65 for geopolymer formulation (Davidovits 2013).

3 EXTRUSION PRINTING PROCESS

The object, part or structure must be modeled with a CAD software before the physical printing process can begin. The 3D model is then sliced into a wanted thickness corresponding to the layer height usually by exporting the model to another program. From the sliced object data, it is possible to generate g-code which 3D printer reads and prints the object accordingly. The process for 3D printing of concrete-like materials is shown in Figure 4. As seen in Figure 4, the 3D printing process is divided between the software and hardware. Nozzle movement is enabled with the 3D printer itself, which type can vary. All 3D printers that print concrete-like materials require a material delivery system that combines from mixer, pump, hosing and piping. The integrated controller must control the movement of 3D printer and speed of the pumping according to the design of the object. (Paul et al. 2018a)

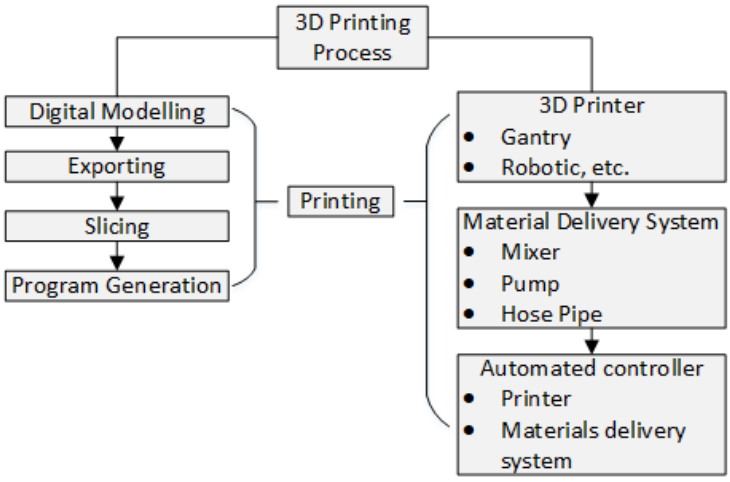

Figure 4. 3D printing process of concrete-like materials in general (Mod. Paul et al. 2018a).

The geopolymer printing process can be divided into three main areas: geometry and size of the component, material parameters and machine parameters. Most important material parameters are open time and properties that affect on pumping and buildability. Machine parameters (pressure, speed, layer height) needs to be set according to the material properties and the geometry of the component. The material must be selected based on the component to be 3D printed or vice versa. (Panda et al. 2018b) The triangulation between the component, material and machine parameters is presented in Figure 5.

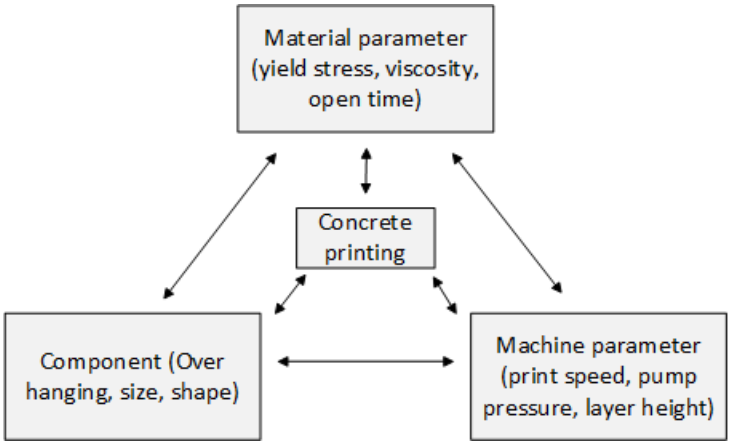

Figure 5. Main areas that need to be considered in 3D concrete printing (Mod. Panda et al. 2018b).

Key for successful printing of geopolymer materials is highly affected by the composition of the geopolymer. 3D printable materials require stable and repeatable open time, in which the material is workable, pumpable and buildable. High yield stress is required from the material, yet the material needs to become less viscous while agitated and turn back to initial state after extruding. Bonding of printed layers must be possible during a long period to maximize the operation window. The design of the object or structure to be 3D printed has an impact on the success of the print. (Buswell et al. 2018) Material affects the required printer design and the design of the object to be 3D printed (Ma et al. 2018b). A more detailed presentation of correlation and requirements for material and printer design is illustrated in Figure 6.

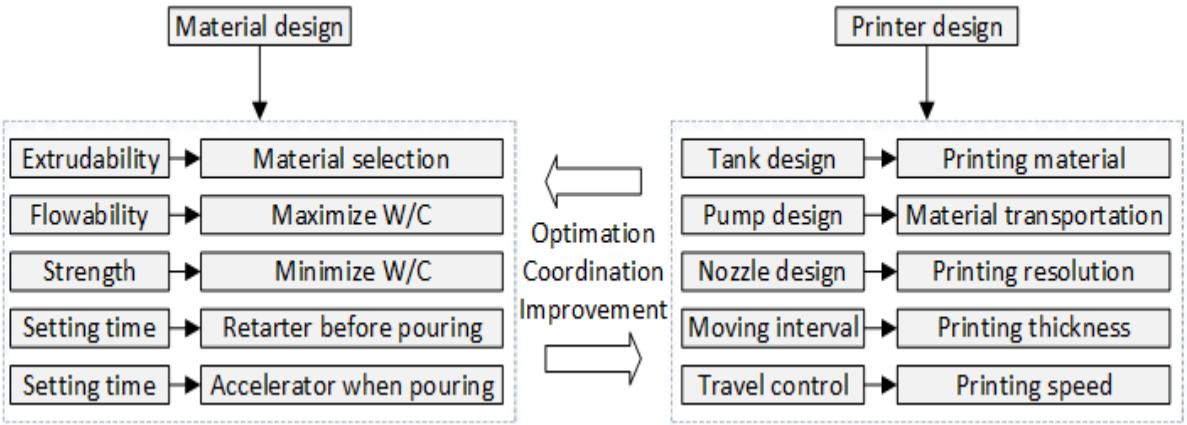

Figure 6. Correlation between the printer and material design and general requirements for mix design (Mod. Ma et al. 2018b).

Geopolymer to be printed can be described on its pumpability, extrudability and buildability which are strongly related to each other. Structures and components can be printed vertically or horizontally. Vertically it is possible to print complete houses or other large objects, while horizontally printed parts are usually elements that can be used to assemble structures or other items. (Buswell et al. 2018)

3.1 Material mixing, preparation and batching

According to several studies, dry materials are usually mixed together for 1–3 min in a mixer, for example, planetary or Hobart mixer. The alkaline reagent of some sort (Table 4) is usually mixed next for 1–2 min. Both mixing processes can happen in the same mixer or they can be mixed in separate mixers. Sand can be mixed same time with the precursors (fly ash, slag and silica fume etc.) or they can be added after the alkaline reagent for mixing additional 1–2 min. Thixotropic additives can be mixed with dry materials to achieve extrudable geopolymer. (Nematollahi et al. 2018, Panda et al. 2018b, Al-Qutaifi et al. 2018) Lastly, water can be added slightly to improve the workability of the geopolymer in the printing process. Different factors can affect the properties of geopolymer after extrusion for example pump pressure, hose length and geometry of nozzle. (Panda et al. 2017b)

The size of the material batches for the printing process is dependent on the size and geometry of the component to be printed which affects directly to the deposition rate needed. Batching can be done in larger or smaller amounts called conventional and micro-batching. It also could be possible to mix the materials directly at the deposition head. The size and type of mixer affected by the previously mentioned factors. (Buswell et al. 2018) In studies, usually one batch size is mixed and then the open time is investigated (Kashani & Ngo 2018, Panda et al. 2018b, Panda & Tan 2018, Panda et al. 2017b, Paul et al. 2018a, Panda et al. 2018a, Lim et al. 2018).

3.2 Rheology

Properties of fresh geopolymer can be measured using the rheological measuring devices. Yield stress and plastic viscosity of fresh geopolymer mix are important for the printing process because they are related directly to hardened properties and printing quality. Thixotrophy property is critical for the success of the print. High yield stress and low viscosity are the key material properties for the extrudability and maintaining stability.

Certain concrete dependent shear stress is required to make the fresh material flow which correlates with the yield stress. Resistance to the flow is measured with plastic viscosity after the flow is initiated. (Panda et al. 2017b) The changing rheology for geopolymer during the time is tracked by performing the test in suitable time intervals. Yield stress and viscosity (Bingham parameters) can be determined and shear stress, static yield stress and viscosity calculated. (Panda et al. 2018b) Rheometer is commonly used for the rheology measurements. Vane probe with four blades is immersed in the material. Vane probe starts to rotate in the material at increasing speed to 60 rpm in 2 min time span. The rotation is kept constant for the following 2 minutes and finally reduced to zero in the next 2 minutes time. Graph of torque and rotation is generated where thixotropy can be measured and Bingham parameters calculated. (Panda et al. 2018a)

3.3 Open time and workability

The fresh properties, especially flowability of concrete-like materials change with time. Open time refers to the time frame on which the material remains workable so that it can be pumped and extruded to form a consistent printing quality. This includes viscosity and yield stress of the fresh material, which must be maintained and can be measured with a rheometer. (Paul et al. 2018b) Different components to be printed require different open time for printing. Printed material may need to be formulated or selected to the specific application. (Buswell et al. 2018) Typical open time range for geopolymers have been reported to be 30 min to max 60 min, 45, 20 and 30 minutes (Paul et al. 2018a, Kashani & Ngo 2018, Panda et al. 2018b, Panda & Tan 2018).

Open time of cementitious 3D printable materials can be estimated with different test methods if rheometer is not used. Open time of the material can be tested with a setting time test utilizing Vicat apparatus. The Vicat test gives an approximate time for open time since it does not measure the physical properties of materials. Slump test can be used for measuring open time property of shear stress indirectly. (Paul et al. 2018b, Le et al. 2012b) Slump test gives slump value and the change of the value can be used for estimating workability of material. Slump test is also not able to measure real values of stress or viscosity. (Le et al. 2012b) Mentioned testing methods have their own national standards, for example, Vicat test and slump test have standards SFS-EN 193-3 and SFS-EN 1015-3 respectively. Mentioned procedures are described more precisely in chapter 5.

3.4 Pumping and pressure

Fresh geopolymer mix is usually transported from material container to the extrusion nozzle using a pump. To describe how easily the fresh mix can be pumped, the term pumpability is used. (Buswell et al. 2018) Pumpability can be also described as the material behavior under pressure in terms of stability and mobility while initial properties of the material are maintained (Paul et al. 2018b). Hoses are usually used to transport fresh material to the nozzle. The fresh mix transportation through the hose can result in blockages due to insufficient mixing or mix design. Positive displacement pumps are used to minimize possible blockages. Design of the fresh material mix can be made so that it has lubricating properties inside the delivery hose or pipe. Blockages are also highly dependent on the yield stress of the extruded material. (Buswell et al. 2018) For efficient pumping, the material mixture should be designed for pumpability in mind. Material should be soft while pumping and in the extrusion phase, it should be stiff enough to stay in shape. Paste content in the mix should be sufficient for grout form, which can increase the pumpability. High pressures can cause water to squeeze out of concrete materials in so-called bleeding. Material should be designed to resist bleeding with suitable consistency of water and other components. (Paul et al. 2018b)

3.5 Extrusion and layer cycle time

Extrudability is defined from the ability to extrude the material mix without significant deformation, splitting or tearing. Shape, size, movement and position of the nozzle have an effect on the extrudability. (Buswell et al. 2018) Materials are designed with thixotropic features and pumping pressure causes the material to be less viscous due to agitation-reduced viscosity. Nozzle opening size is usually smaller than the pipe diameter, which introduces increased pressure at the nozzle, which can make material stiffer and enhance shape retention and stability. Segregation may happen in extrusion and nozzle or pipe can be blocked if the material composition cannot handle the pressure changes while it is extruded. (Paul et al. 2018b)

The time between when a layer is extruded on top of a previous layer in the same location is described as layer cycle time. Layers are printed in vertical height and the path of each layer is repeated mostly similar or identical to previous. Path length caused by the geometry of

object being printed and extrusion speed for the material are important factors for the interlayer bonding and its strength properties. The cycle time can lead to changes in material properties between the layers. Proper layer cycle time is crucial for layer adhesion. Layer does not bond well if the layer cycle time is too great for the material. The effect of layer cycle time is significant for strength properties of the final printed object, which requires layer cycle time to be considered in the design phase of objects possibly with different iterations and simulation models. (Buswell et al. 2018) Layers must be extruded also in the time range that the bottom layer does not collapse or deform under the weight of added layers, which refers to buildability.

3.6 Buildability and printability

Buildability can be used to describe the ability of the material to be self-supportive and retain its shape during the 3D printing. Buildability, like other 3D printing characteristics, can be improved by tuning the material properties. Nozzle shape and type will affect buildability. Layers extruded with round nozzle have less contact area compared to square or rectangular nozzle, which can lead to a poor buildability as layers increase. Printing of layers adjacent to each other will improve buildability before printing upwards. Previous method has limitation depending on the required object wall thickness and material open time. (Paul et al. 2018b)

Shape retention or stability refers to the shape changes of the material after extruding, which is highly related to printability, but also to buildability of the material (Panda & Tan 2018, Kazemian et al. 2017a). Material with low slump and high yield stress will keep its shape better than the material with opposite characteristics. The yield stress of the material cannot be too high, or the material is no longer extrudable. Shape retention factor (SRF) can be calculated which describes the material ability to retain its shape and it has correlation with a yield strength of the material. (Panda & Tan 2018) Stability is also affected by the layers that are extruded on top of each other including the own weight of the layer, and the extrusion pressure. Required stability must be determined based on the object that is 3D printed. (Kazemian et al. 2017a)

3.7 Quality

Quality can be inspected visually when it comes to extrusion. For strength and other physical properties, different testing methods are needed. More weight and hydrostatic pressure will build up on top of previous layers as the printing process advances. Layers compress under the weight of the top layers, which can lead to problems in extrusion as the shape of layer can change. If the compression is not compensated, the nozzle distance to the previous layer increases and can affect the layer adhesion. The effect gets worse as the printing continues and can ultimately lead to a collapse of the structure. Some deformation can be applied when adding the upper layers on top of the previous layers to achieve better adhesion, but without dynamic adjustment problems described above may occur. (Buswell et al. 2018)

Voids can be created inside the component, which can be referred to as under-filling. The durability of the printed component is potentially worse with voids. Voids can be avoided with proper mix design and rheological properties which will have an effect on the extruded layer shape and size. The print path can also affect the density of print. (Buswell et al. 2018) Density can be higher in printed components compared to casted ones due to pumping pressure in the extrusion phase (Panda et al. 2017b).

4 STRUCTURE OF PRINTERS

Most of research and development in the field of concrete 3D printing has been carried out in commercial organizations. Universities and institutes have not researched the topic widely and the amount of research papers is limited. (Paul et al. 2018a) Concrete based 3D printing has been developed mostly over the last ten years and research is done worldwide by more than 30 groups in commercial companies and in universities (Buswell et al. 2018). Printer solutions can be divided into three main categories: gantry, robotics, and crane (Paul et al. 2018b). Some more rare solutions are cable suspended and swarm (Labonnote et al. 2016). In Table 5 some companies and institutions are listed that work on extrusion 3D printing of concrete or cementitious materials.

Table 5. List of companies/ institutions that make/ develops extrusion-based 3D printers for concrete or cementitious materials (Delgado Camacho et al. 2018, Lampinen & Alonen 2017).

Company/ institution	Year	Printer type
Apis Cor	2015-	Crane
BetAbram	2012-	Gantry
Contour Crafting corp.	1998-	Gantry
Constructions 3D	2016-	Robotic crane
CyBe	2013-	Robotic arm
Danish Technological Institute	2016-	Robotic arm
HuaShang Tengda	2016-	Gantry
IAAC (The Institute for Advanced Architecture of Catalonia)	2002-	Robots, Swarm
Loughborough University, Forster & partners, Skanska	2007-	Gantry
Lund University	2015-	Gantry
Spetsavia	2015-	Gantry
Total Kustom	2014-	Gantry
TU/e (Eindhoven University of Technology)	2015-	Gantry
Win sun (Ying chuang)	2004-	Gantry
XtreeE	2015-	Robotic arm

Only the company Apis Cor has been reported to utilize its machinery in 3D printing of geopolymers (Lampinen & Alonen 2017).

4.1 Machine structure

Studies usually describe the structure of the AM machines used for the research briefly. No proper mention is made on how the machine structures were developed and how components were selected. Used printers are typically scaled to manufacture test samples for investigation of print quality and other properties seen in studies of Panda et al. (2017a, 2017b, 2018a, 2018b), Paul et al. (2018a), Nematollahi et al. (2018) and Ma et al. (2019)

Printer setups consist of the same main components. Tank or container is used to store fresh mixed material. Pump is used for pumping the material to the moving print head and nozzle. Pipes are used between the pump and printer head and nozzle assembly to transport the printable material. Movement of the printer head is controlled by a controller. The machine must move in X, Y and Z directions to be able to print 3D components. (Ma et al. 2018b) In laboratory scale tests material can be stored in a tank above the extrusion nozzle mounted on the printer head (Le et al. 2012b).

In Figure 7 example of the setup for 3D printing concrete in the laboratory scale is presented. Robotic arms can be programmed to perform the path needed for the component construction. Other functions to the mere extrusion could be added for the robotic arm configurations, for example, painting and placing of reinforcements. Typically, robotic arms have 5 or 6 axis of freedom in the 3D printing applications. (Labonnote et al. 2016) The freedom of movement allows more complex geometries to be 3D printed compared to gantry solutions with 3 or 4 axis (4^{th} axis being the possible rotation of the nozzle or printhead). When complexity is not required in the printing of objects gantry solutions are more reasonable and cheaper compared to robotic solutions. (Paul et al. 2018b)

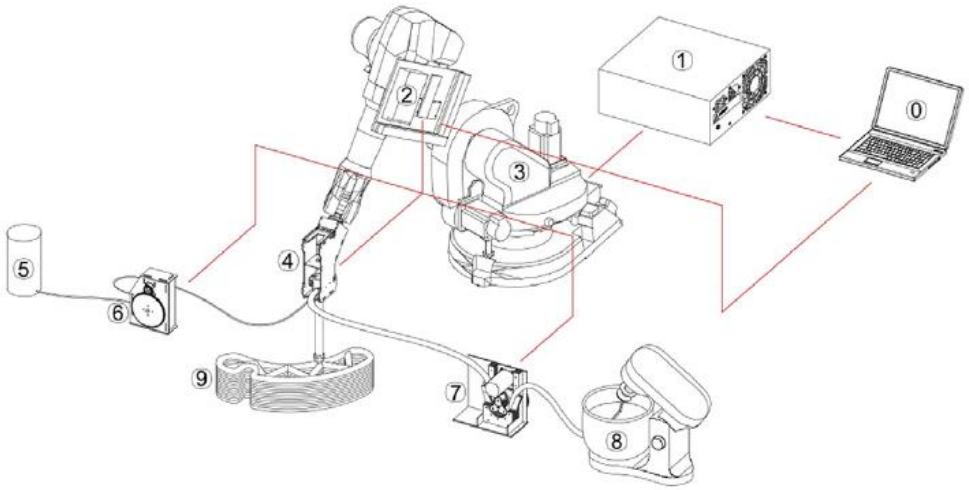

Figure 7. 3D printing setup with a robotic arm for concrete materials in laboratory scale (Gosselin et al. 2016).

According to Gosselin et al. (2016), the setup in Figure 7 consists of: "0. System command; 1. Robot controller; 2. Printing controller; 3. Robotic arm; 4. Printhead; 5. Accelerating agent; 6. Peristaltic pump for accelerating agent; 7. Peristaltic pump for premix; 8. Premix mixer; 9. 3D printed object." With setup where chemical additives are mixed just before the nozzle in printer head allows lower viscosity material to be mixed at the mixer, which makes the material easier to pump (Paul et al. 2018b). In Figure 8 similar setup as in Figure 7 is presented in a larger scale with the difference in mixing and pumping all ingredients in stages before the nozzle. Robot printers typically have limitations in scalability of the printer, and it can handle lower payloads compared to gantry printers. (Paul et al. 2018b)

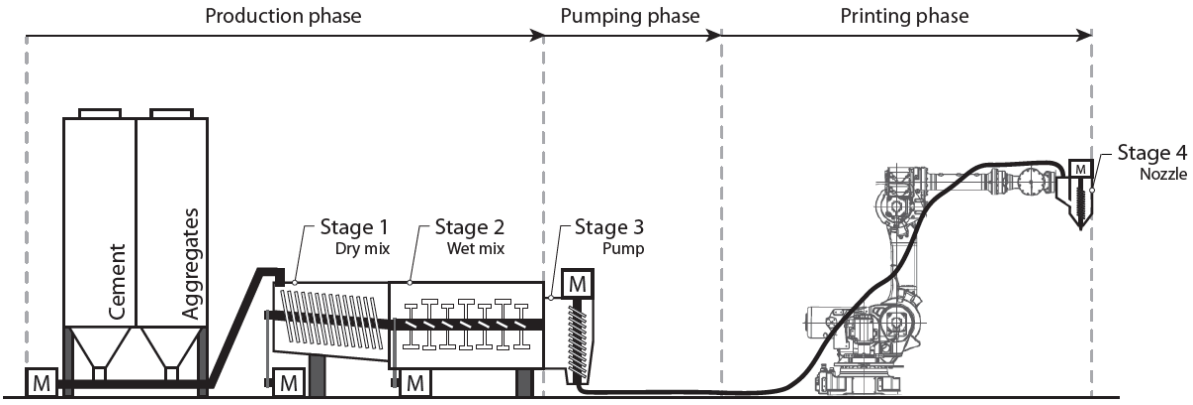

Figure 8. 3D printing setup with continuous mixing and feedback system (Mod. Leal de Silva 2017).

Gantry systems used in a concrete 3D printing can be constructed from a steel frame shape of a cube. The print head is moved from the top of the frame with three beams in the dimension in order to build 3D objects. (Le et al. 2012b) The gantry solution could be described as a scaled up FDM (fused deposition modeling) printer. The printing head is controlled in X, Y and Z directions in Cartesian coordinates driven by numerically controlled actuators. (Paul et al. 2018b) In Figures 9 and 10 different sizes of gantry solutions are presented.

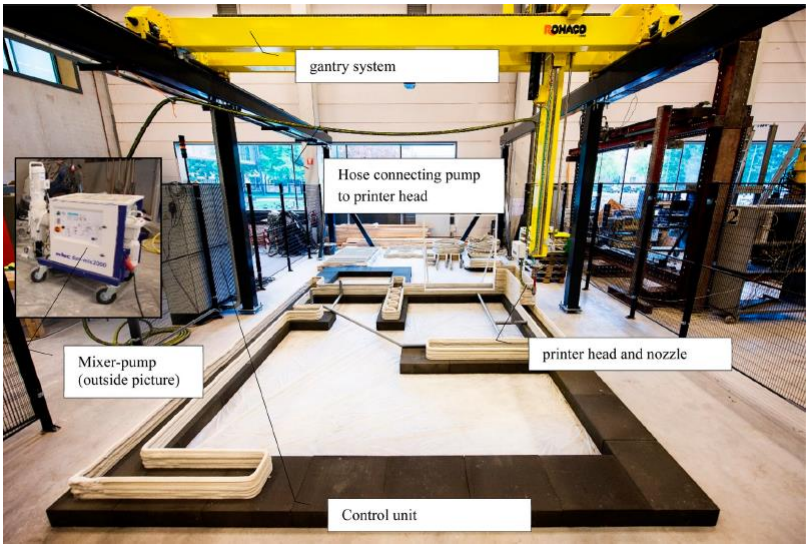

Figure 9. Example of a 3D printing system in TU Eidenhoven (Bos et al. 2016).

The gantry 3D printer in Figure 9 has printing area dimensions of 9 x 4,5 x 2,8 m. The material is delivered by a pump to the printer head through a hose. Control unit controls both the pump and gantry system. (Bos et al. 2016)

Figure 10. Laboratory scale gantry style printer and pump setup (Lao et al. 2017).

Laboratory scale gantry printer in Figure 10 has dimensions of 1 x 1 x 1,2 m in the printing area and the material is delivered through 25 mm diameter hose pipe (Panda et al. 2018b). The hosepipe is up to 3 meters long and the material is pumped with a cavity pump (Panda et al. 2017a). In Figure 11 crane 3D concrete printer solution is presented.

Figure 11. Crane 3D printer by Apis Cor. Material mixer and pump are not part of the crane. (Apis Cor 2017)

Crane solution can be easier to transport if on-site printing is utilized. Crane printers have an advantage on the gantry in size. With gantry solutions, frame size is fixed but with a crane the arm extends and tower can rise the needed amount while printing the object. (Paul et al 2018b, Ghaffar et al. 2018)

4.2 Mixers

It is important for the end result of concrete material that the mixing procedure is well managed which includes the correct order of ingredients added to the mixer, duration and power of mixing (energy) and the type of mixer itself. In concrete applications, mixers can work on two principles by producing batch or continuous mixing. (Ferraris 2001)

Batch mixers can mix a fixed amount of material depending on the mixer size. End of mixing, the batch mixer is emptied and cleaned which allows the next cycle of mixing to begin. Batch mixers are classified as a drum mixers with a horizontal or inclined axis of rotation and as a pan mixers with a vertical rotation axis. Mixing is performed by blades and rotational movement. In drum mixers, the drum rotates around fixed blades. In pan mixers,

there is one or two set of rotating blades and the cylindrical pan itself can be rotating or fixed. (Ferraris 2001)

Continuous mixers mix and discharge the material continuously at the same rate. Mixers that work with continuous mixing principle are suitable for low slump concretes, where working time is limited. The mixing time in continuous mixers is shorter than in batch mixers. Mixing is usually separated to dry and wet mixing wherein the former materials are mixed before introducing any liquids. After dry materials are thoroughly mixed liquids can be added and mixing has turned into wet mixing. Dry ingredients can be still added to the wet mixture during mixing. (Ferraris 2001)

Mixing of the printable material usually happens in stages. All the material that is needed for the printing of an object usually cannot be mixed at once. New fresh material is mixed as the material reservoir is getting empty which creates a variation on the printable material age, and the pressure must be controlled accordingly. (Bos et al. 2016) Figure 12 shows three different mixers for geopolymers and concrete. Traditional concrete mixers can be used for geopolymer mixing (Paul et al. 2018a).

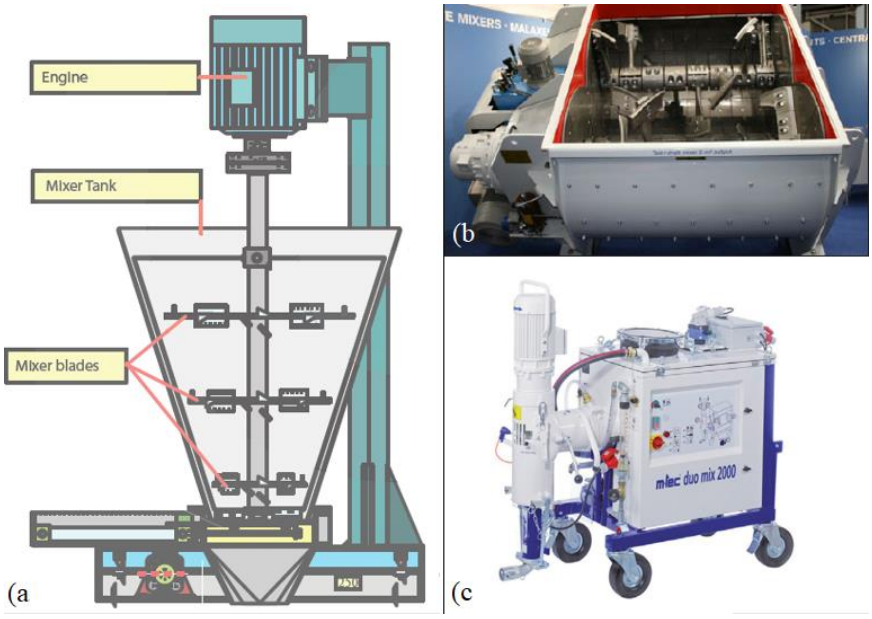

Figure 12. Three configurations for mixing concrete and geopolymers. a) Schematic of mixer for 3D printable geopolymer (Renca 2018). b) Mixer with horizontal twin shafts (BMH systems 2018). c) Mixer and pump combination (M-tec 2018).

The mixer can be part of a larger system with automatic transport of ingredients to the mixer and pumping to the printer as seen in Figure 13. Mixer can also have automatic cleaning between the batch mixing. (Renca 2018) Mixer unit can be mobile and have a pump integrated directly to it (M-tec 2018).

Once the material is mixed and ready to be extruded the material properties are hard to control. Material cannot be mixed after it leaves the mixer and if printing is non-continuous the fresh properties of the material will change during printing. Some configurations can have a mixing screw on print head in order to mix accelerating agents as late as possible before extrusion (Gosselin et al. 2016).

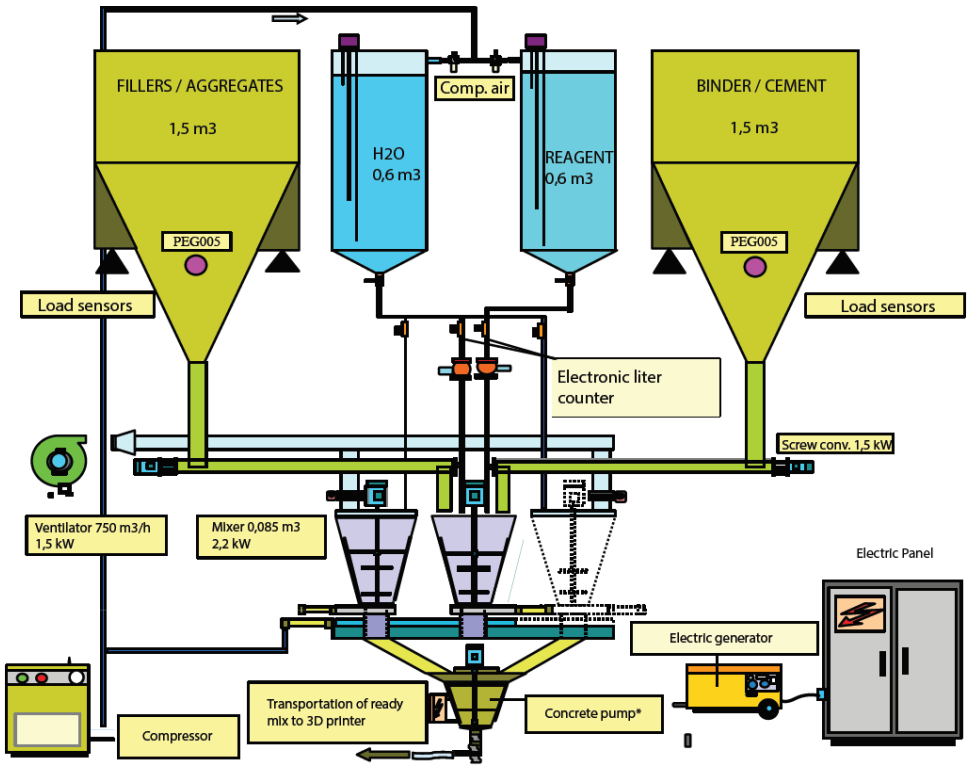

Figure 13. Automatic mobile mixing plant for 3D printable geopolymers (Renca 2018).

Sizes of mixers vary depending on the manufacturer. The mixer should be selected according to the printer application. Mixer system from Renca has two mixers size of 0,085 m^3 (Renca 2018). In laboratory scale, Hobart mixers and high shear planetary mixers have been utilized (Lim et al. 2018, Panda et al. 2017b).

4.3 Pumps

Studies of pumps used in concrete industry and 3D printing applications where searched in order to find reference of types of pumps that are used or could be used in 3D printing of geopolymers. Material needs to be transported from the mixing unit to the nozzle and pumps are utilized for that purpose (Paul et al. 2018b). In concrete construction, large-scale pumps are utilized. Most common type pumps for concrete are piston pumps/ high-capacity dual-piston pumps (Riding et al. 2016).

In 3D printing applications, no mention of the use of above-mentioned pumps were found. Pumps that are used for concrete pumping should withstand abrasives of the material to be pumped. Maintenance should be guaranteed for the pump in case of high wear. (Labonnote et al. 2016) Pump types that are utilized in concrete 3D printing are commonly positive displacement pumps (Buswell et al. 2018). Peristaltic pumps are utilized in some studies, even though they have pulsating flow, while constant flow is usually required for proper extrusion (Gosselin et al. 2016). Progressive cavity pumps, peristaltic pumps, screw pumps and piston pumps work on the principle of positive displacement where the amount of substance is moved when it is trapped and forced by the movement to the discharge pipe or tube. Cavity expands on the suction side and decreases on the discharge side, which makes the pumped substance to flow in constant volumes. (Pump 2011) In Figure 14 typical progressive cavity pump is shown.

Figure 14. Progressive cavity pump and its main parts (Leal de Silva 2017).

Progressive cavity pump has a helical shaped rotor which is fitted inside shaped rubber sleeve. High pressures can be developed with the pump for even low volumes. Peristaltic

pumps use flexible tube and as the circular rotor turns the rollers on external circumference compresses the tube. Tube closes partly, and trapped substance is forced through the tube to the discharge end. Screw pumps have usually two or three intermeshing screws rotating opposite directions due to opposing threads. The rotating movement forces material through the pump with the moving cavities created between the two screws. Screw pump with single screw is used for high solid content material pumping. (Pump 2011) In laboratory scale, pumping can be done by piston-type configuration where the material is placed in a cylinder and pressed with a piston in order to extrude the material. (Sanjayan et al. 2018, Kazemian et al. 2017a)

Pumping pressures have been reported in some studies. Pressures used for geopolymer pumping where fluctuating between 10 and 15 bar in studies (Panda et al. 2017b, Panda et al. 2017a). Pump pressure range can also be from 4–10 bar during the printing process (Paul et al. 2018a). Highest found pumping pressures are reported to be high as 10 to 40 bar (Paul et al. 2018b). Commercial printer manufacturer Apis Cor and pump and mixer manufacturer M-tec have pumps capable of max. 30 bar pressure (Apis cor 2017, M-tec 2018).

Pumping pressures for 3D printing have been obtained by empirical testing. For pumping of concrete materials, some theoretical models have been developed. These prediction models of pumpability are made for pumping circuits of length of 200–1000 meters. (Kim et al. 2018) Pumping distances in 3D printing have been significantly less. The printer of Apis cor reports max. 80 m distances and 30 m distance in height (Apis cor 2017). M-tec promises to pump 60 m horizontal and 30 m vertical distances (M-tec, 2018).

Correct pump pressure can be hard to determine. Pressure is dependent on the fresh material properties and the change of properties during printing. Yield stresses of material to ensure pumpability in order that blockages do not form, and extruded layer stays intact have been reported to be in range 0,3–0,9 kPa. (Buswell et al. 2018) Pumping speed needs to be adjusted depending on the geometry of the printed object. While printer head moves through corners it needs to decelerate which means that pumping speed needs to be reduced at the same time. Discontinuities introduced by the geometry of printed object requires the extrusion to stop from time to time. This requires controlling not only pumping but nozzle speed and rotation as well at the same time with one control unit. (Paul et al. 2018b)

Maximum pumping speeds can vary. Apis cor reports pumping speeds max. 30 l/min (Apis cor 2017). M-tec list average pumping speed 22 l/min (5–60 l/min depending on the pump) (M-tec 2018).

4.4 Printer heads and nozzles

Printable material exists the printer system through the nozzle. The main purpose of the nozzle is to deposit the material evenly on layers and give the extruded layer its shape. There are mainly four types of nozzles used for the extrusion: round, ellipse, rectangular and square. (Paul et al. 2018b) Rectangular nozzle must be able to turn and move tangent in curves to avoid problems in extrudability. Round nozzle does not require additional turning in the print head, which makes it simpler compared to the rectangular. (Bos et al. 2016)

Nozzles have been studied mainly by the shape of the orifice and how it affects the quality of the extruded filament. Design and shape of the nozzle have an impact on the compactness and surface finish of printed part or structure. By optimizing the nozzle shape compactness, surface finish and mechanical strength can be improved. (Lao et al. 2018) Round nozzles extrude layers that have an elliptical cross-section, which creates voids in printed structures if the material is extruded side by side. Rectangular nozzle with optimized shape will have fewer voids than the round counterpart, and more contact area with the bottom and adjacent layers. (Lao et al. 2017)

Size of the nozzle is selected based on the component to be printed. The shape of the printed object or component can also influence the shape of the nozzle to be selected. Rectangular nozzles have commonly varied between sizes 9x6 to 38x15 mm. (Paul et al. 2018b) Round nozzle orifice size typically varies between 6–50 mm in diameter. The extrusion quality is usually evaluated visually to check any deformation, splitting and tearing of the extruded filament. (Buswell et al. 2018)

Surface finish of printed structures can be enhanced with applying trowels outside the nozzle. The outer surface of the extruded material is shaped with the trowel or trowels to achieve better surface quality and layer adhesion. (Hwang & Khoshnevis 2004) Nozzles with trowel solutions are presented in Figure 15.

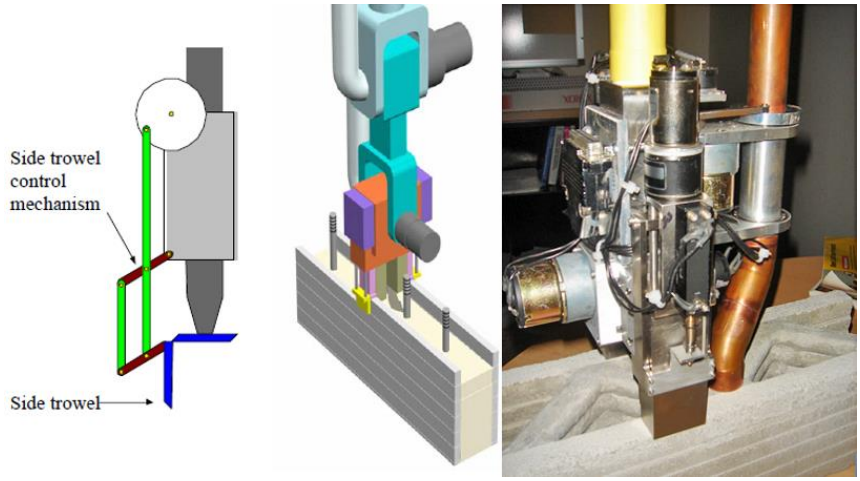

Figure 15. On left nozzle assemblies with trowel mechanisms (Hwang & Khoshnevis 2004). On right real nozzle assembly for printing wall with two sides and corrugated fill (Abrams 2014).

The technology of the printer heads shown in Figure 15 is called contour crafting (CC). Characteristic for CC machines is the use of trowels and possibility to add constructional elements, for example, enforcements, plumbing and electrical to the printed wall structures. Freeform is not possible with CC since the nozzle type is made for specific wall element printing. Many of the CC solutions are patented under the name contour crafting which may limit the use of the solutions commercially. (Labonnote et al. 2016) In Figure 16 typical nozzle solutions are presented.

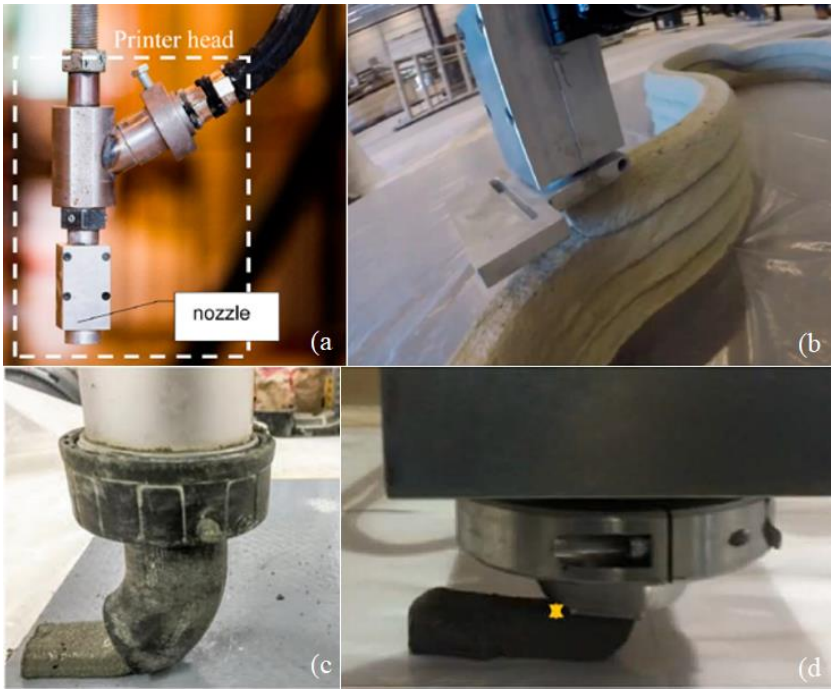

Figure 16. Head and nozzle assembly of four different printers presented in studies. a), b) Printer head and the nozzle are illustrated with two different sizes and shapes (Bos et al. 2016). c) Nozzle with a rectangular opening in a 45-degree angle (Nematollahi et al. 2018). d) The nozzle of a laboratory scale printer (Panda et al. 2018b).

Nozzle is usually made of steel or equivalent hollow element with a shape that is commonly round or rectangular (Bos et al. 2016). In Figure16c it is visible, that printer nozzle could be PVC-plastic material. Printer nozzles have been also made from plastics by extrusion AM. In studies of Lao et al. (2017) and (2018) nozzles with shapes of round, elliptical and rectangular were printed with FDM (Lao et al. 2018, Lao et al. 2017). Danish Technological Institute has also 3D printed nozzles of different shapes for the concrete printer (Leal de Silva 2017). In Figure 17 some commercial nozzle solutions are shown.

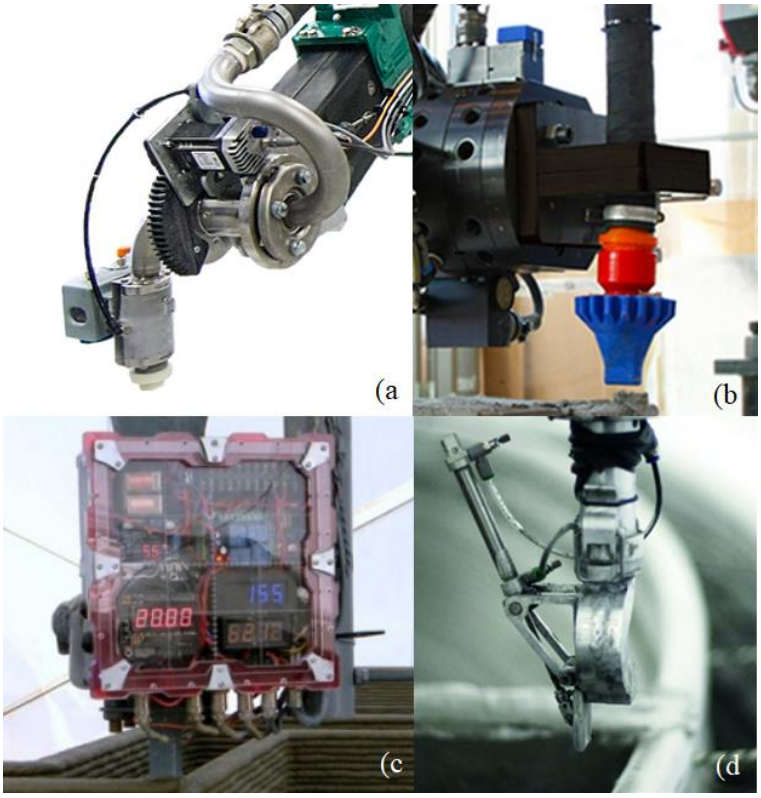

Figure 17. Four printer heads and nozzles from different makers. a) Turning printer head in the printer of company Constructions 3D (Constructions 3D 2018). b) Extrusion nozzle in printer made by Danish technological institute (DTI 2018). c) Printer head and nozzle of company Totalkustom (Totalkustom 2015). d) Nozzle with side trowel in the printer of company Apis Cor (Cusack 2018).

Most of the printer heads nozzles seen in Figures 16 and 17 are passive meaning that the nozzle dispenses the material and is controlled by a pump from a distance. In Figure 17c the printer head and nozzle can be called active as the pump is located at the printer head which enables precise control and admixtures. (Leal de Silva 2017) Vibration can be applied to the print head to guarantee the compaction of the mixture before extrusion (Nematollahi et al. 2018).

5 TESTING OF PRINTABLE MATERIAL PROPERTIES

Printed objects can be similar in strength properties compared to casted counterparts. In large and commercial scale equal to casted properties in printed objects has not been achieved yet. Printed objects still have anisotropic property because objects are built in layers. (Buswell et al. 2018) Standardized testing methods have not been developed for 3D printable geopolymers or concrete. Lack of testing guidelines makes it harder to compare and model the mechanical properties of the 3D printed elements. There is no agreement on the size of the printed object for testing and objectively characterize the mechanical properties. Guidelines could be created for tensile bond, flexural and compressive strength testing. The layer or interface minimal amount for testing is yet to be clarified. (Paul et al. 2018) Testing is divided into fresh state material testing to determine material suitability for the overall 3D printing process, and hardened state material testing to test the performance of the final 3D printed object.

5.1 Setting time

Setting time can be determined according to tests described in standard SFS-EN 196-3 (2016). The test utilizes Vicat apparatus in which needles vertically penetrates the paste under a total mass of 300 g. Initial and final setting times are determined between the time of when the material is mixed and when the needles do not penetrate the paste over a certain amount. The distance between the needle and the base where paste lies on is measured at time intervals convenient for the material, for example, 10 min intervals. Initial setting time needle is length of 45 mm and diameter of 1,13 mm. After the initial setting time is reached, final setting time can be measured by inverting the paste sample and repeating the measurements with a needle which has a 5 mm diameter ring attached on the tip. (SFS-EN 196-3 2016) In the study of Kashani & Ngo (2018), initial setting times for different geopolymer paste mixtures were measured with the Vicat needle according to the standard procedure. Higher amounts of reagents in the mixture can lower the initial setting time up to six times because of higher dissolution of particles and pH and faster reaction.

Another standard way of testing setting time of concretes can be done according to ASTM C403/C403M-08 (2008) which is similar to the Vicat test. The test utilizes a needle with a

bearing area between 645–16 mm^2. The needle is connected to a penetration resistance apparatus, which can record the used force and is then penetrated into the mortar to 25 mm depth with constant speed in selected suitable time intervals. Penetrations (minimum amount 6) are continued until there is no space for measurements to be taken or until force of 27,6 MPa is exceeded. Initial setting time is reached at 3,5 MPa. (ASTM C403/C403M-08 2008) The test has been performed for 3D printable concrete by Kazemian et al. (2017a). With both methods, a curve from the setting development can be plotted from which the setting time can be analyzed.

5.2 Slump and shape stability tests

Slump test is utilized to describe workability and flowability of the cementitious or concrete material, lower value means less workable (Al-Qutaifi et al. 2018). The test is performed with filling a cone-shaped mold in layers and tamping the material to the mold. The face of the cone mold is smoothened, and mold removed. The table that the material rests on is jolted in constant frequency. Material spreads on to the table and the diameter is measured. Relative slump value can be calculated based on the results. More the mortar spread the higher the value. (SFS-EN 1015-3 1999) Traditional slump test has been conducted according to national standards in studies related to 3D printing of geopolymer by Al-Qutaifi et al. (2018) and Paul et al. (2018a).

Shape stability is similar to the slump test where the fresh material strength and self-supporting characteristics are measured. Material is poured and damped usually to a cylindrical mold and then the mold is removed and the change in height is measured. Pressure can be then applied on top of the material to test how it can sustain the weight of layers that will be printed on top of the material. Interval of weight addition and the applied force is dependent on the application, which must be determined for each specific printing purpose by calculating layer height and printing speed. (Kazemian et al. 2017a, Panda & Tan 2018) A similar procedure was described in the study of Panda et al (2017b) called plate stacking test, where plates were used as weights to simulate the next layers. Stability can be determined also with single weight addition on top of material as it correlates with a test of interval weight addition (Kazemian et al. 2017a).

5.3 Temperature and heat

Geopolymers have different properties compared to OPC. Durability, mechanical and thermal properties can be better for geopolymers than OPC depending on the chemical composition of ingredients. Disadvantages for geopolymers are generally faster setting time, higher shrinkage than in OPC and the need for curing in above room temperatures. Need for curing in elevated temperatures can be avoided with calcium enriched ingredients and use of suitable aluminosilicates. (Panda et al. 2018a)

Geopolymer test samples have been mechanically tested after curing in the oven and curing in ambient room temperatures. Best result from oven curing can be achieved by delaying the start up to five days. Alumina and silica have time to dissolve in room temperature before the oven, which will enhance the geopolymerization process. The geopolymerization process is accelerated in temperatures between 60–80 °C, above 90°C temperatures can have a negative impact on mechanical properties of geopolymer. Dry-curing results in higher strengths in geopolymers than steam-curing. (Al-Qutaifi et al. 2018) Ambient curing in room temperature usually requires 28 days of curing in order to achieve the same mechanical properties as 24 hour oven cured samples (Nematollahi et al. 2018).

5.4 Testing of hardened material properties

Properties of printed objects are usually tested by printing block or slab from which cube specimens are extracted. Testing is made for specimens that have cured different time periods, usually 7, 14 and 28 days. Testing is made also with specimens with different layering time in order to investigate the bonding of layers. All tests can be made for the specimens from three different directions to test the anisotropic nature of printing shown in Figure 18. (Le et al. 2012a) Geopolymer properties can be tested according to SFS-EN 12390 standards for testing hardened concrete. SFS-EN 196-1 methods of testing strength of cements or equivalent standards have been also used for geopolymer hardened properties testing.

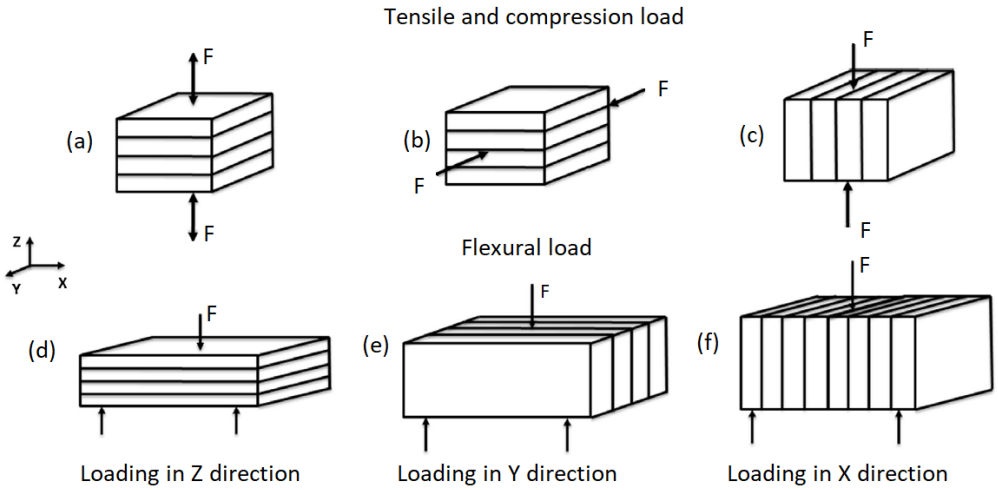

Figure 18. Load directions for 3D printed objects related to the printing direction (Mod. Paul et al. 2018a).

Prior to implementing formulated geopolymer to 3D printing tests, laboratory test with molds can be made. Layering process of 3D printing can be simulated with a mold system that can be stacked on top of another mold. (Al-Qutaifi 2018) For testing of setting time, slump or hardened properties, standards have their own sample sizes and molds.

5.4.1 Interface strength of layers (bond strength)

Layer by layer method in 3D printing means that material that is being applied on top of the previous layer should form a bond to it in order to ensure the strength of the printed component. The interface strength can be considered one of the most important factors in 3D printed structures for guaranteeing stability. (Panda et al. 2018b)

Testing of interface strength between old and new concrete can be performed with several different test methods, principally shear, tension and torsion tests. The values given by the different test may vary measurably depending on the size of the test sample, set-up of the experiment and applied loading rates. (Zareiyan & Khoshnevis 2017) Figure 19 presents 6 different methods for testing of bond strength.

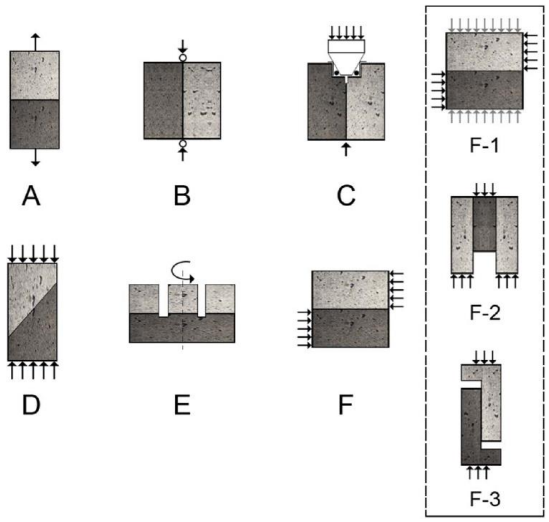

Figure 19. Methods for testing bond strength of layered concrete. A: pull-off, B: tensile splitting, C: wedge splitting, D: slant shear, E: torsion, F: parallel to the interface. (Zareiyan & Khoshnevis 2017)

Bond strength between the layers is commonly determined with pull-off test, even though the test results can vary depending on if the applied load is not perpendicular to the test specimen interface. The stress test should be chosen according to the stress condition that is most likely affecting the printed structure. (Zareiyan & Khoshnevis 2017) Tensile bond strength is tested for example by Panda et al. (2018b, 2017a, 2017b), Nematollahi et al. (2018), Le et al. (2012a) and Zareiyan & Khoshnevis (2017) with different methods and specimen sizes. There are few standards that have been utilized in the testing of tensile strengths that are not designed for 3D printed samples.

Concrete tensile strength can be measured with a tensile split strength test where a cylindrical test sample is compressed along narrow region on the length. This creates an orthogonal tensile force to the specimen which ultimately fails under the tension. The test can be also performed for cubic or prismatic specimens. (SFS-EN 12390-6 2010) Size of the test specimens for the previous standard are specified as cubes with a side length of 100, 150, 200, 250 or 300 mm. Also cylinders with diameter same as the cube side length with the addition of 113 mm and length of two times the diameter can be used for testing. (SFS-EN 12390-1 2012) Test by the previously described procedure for cubic specimens where tested by Zareiyan & Khoshnevis (2017). Another method is to drill cylindrical, 50–100 mm in diameter, and length over two times the diameter specimens from a larger sample. Steel

dollies are glued ends of the cylinder and tensile stress test is performed until the specimen fractures. (SFS-EN 14488-4 2008) The test has been utilized by Le et al. (2012a).

Tensile tests have been done also without following any standards. Different sizes of samples for testing are extracted from larger block and sides are glued to a jig which are then attached to a machine for the tensile test. Sizes of 40x40x100 mm, 30x45x160 mm and 25x30x50 mm specimens have been tested for layer bond in tensile test set-ups. (Panda et al. 2018b, Panda et al. 2017a, Nematollahi et al. 2018)

5.4.2 Flexural strength test

Layer behavior of 3D printed geopolymers and similar materials can be tested with three-point bending test. The effect of different parameters to the flexural strength is investigated with different combinations in material composition, layer cycle time and layer patterns. The test specimen is placed on two supports and in the middle of the supports, above the specimen is a third roller. The load is applied to the specimen by lowering the middle roller at a constant speed until specimen fracture. (Al-Qutaifi et al. 2018)

Flexural strength testing can be carried out with standard testing methods developed for cement. Size of the test specimens are 40x40x160 mm prisms. (SFS-EN 196-1 2016) Al-Qutaifi et al. (2018) and Paul et al. (2018a) in their studies have carried out flexural testing according to the previous or equivalent standard. Concrete materials have their own standard for flexural testing. The procedure can be made with two-point loading where the total number of rollers are four, two on top in middle and one on each side. The distance of each roller is equal. The test can be also performed with center-point loading equal to flexural test with cement. (SFS-EN 12390-5 2009) Le et al. (2012a) have tested 3D printed concrete material with the previously described two-point bending test. Test specimens for concrete flexural testing are described in a separate standard. The specimens are shaped as prisms with a width of 100, 150, 200, 250 and 300 mm and length of 3,5 times the width. (SFS-EN 12390-1 2012)

Flexural strength tests have been done with 3D printed specimens that do not follow the dimensions in standards. For example, Nematollahi et al. (2018) and Sanjayan et al. (2018) have made a test for specimens with two printed layers in dimension of 25x30x250 mm.

5.4.3 Compressive strength test

Testing of compressive strength for 3D printed materials can be conducted with standard testing procedures that are developed for concrete and cements compressive strength testing. Hardened concrete has standard SFS-EN 12390-3 (2009) for testing of compressive strength which has been utilized by Le et al (2012a) in their study. Paul et al. (2018a) and Panda et al. (2017a) have tested the printed samples in their studies with standard SFS-EN 196-1 (2016) for determination of strength of cement. Test specimens are applied to a compressive loading in the testing machine designed for the purpose until a failure happens in the test specimen and maximum load sustained is recorded (SFS-EN 12390-3 2009).

Compressive test specimens are usually extracted from the 3D printed slab or another object, which has bigger dimensions than the standard test specimens rather than printing individual samples. Multiple test specimens can be extracted from the slab after hardening. Specimens are usually tested for compression in three different orientations: parallel from top and perpendicular to the layers from both of the sides. (Le et al. 2012a, Paul et al. 2018a, Panda et al. 2017a)

6 MATERIALS AND METHODS

Several different materials and methods were used in the developing and testing phase of geopolymer material. Materials used in 3D printable geopolymer creation and methods used in the fresh material testing and evaluation are based on a systematic approach where the effect of individual components in the material were tested and next steps and decisions were based on results from the previous step. Numerical values were used for evaluating and choosing of geopolymer material mixtures for further testing. Standard procedures were utilized in areas where they have been recognized to be suitable according to other related studies of 3D printable geopolymers. Geopolymer mixes that were numerically most suitable continued to detailed strength tests, and values were measured according to standard procedures which were used for final evaluation of the material suitability for 3D printing applications.

6.1 Raw materials

Raw materials used in this study are composed of materials from local waste and industrial side streams with limited end uses, which often go to landfill. Construction and demolition waste (CDW), bark boiler ash, fly ash, mine tailings and metakaolin are used for the 3D printable geopolymer material development and testing. Commercial sodium silicate solution is used as the reagent for the mix. Bark ash and fly ash that are side products from paper and pulp industry and CDW are main materials for the geopolymer binder formulation. Commercial metakaolin was used as a reactive pozzolan and source of aluminum and silicon. Two different types of sand: coarse and fine were used as filler for the 3D printable geopolymer. The sand used in this study is left over product from mine tailings. Other materials tested for geopolymers as additives were glass wool and carbon fiber. Glass wool has high Si content, which is suitable for geopolymer formation. Recycled carbon fiber had been chopped to 3mm length and it was used to test how it affects the strength properties of the material. Table 6 shows the Al and Si contents of the materials used. Aluminum and silicon appear as oxides in the material and not in pure form. In CDW the variation of content was great between different measured samples.

Table 6. Aluminum and silicon amounts (weight %) of materials used for geopolymer mixture.

Component	CWDs	Bark ash	Fly ash	Metakaolin	Glass wool
Al [%]	8,5 (1,6)	6,5	3,3	21,2	28,9
Si [%]	23,8 (6,9)	6,2	7,6	25,7	1,3

Based on the materials tested in studies on 3D printable geopolymers in Table 3, materials used in this study shown in Table 6 were mixed together to achieve similar Al and Si contents (1,3–2,5). For alkaline reagent sodium silicate solution with a molar ratio of 2,4–2,6 were used (31% SiO_2 and 13% Na_2O). Moisture content of the different industries side stream materials are presented in Table 7.

Table 7. Moisture content of the waste materials.

Material	Fly ash	Bark ash	Sand fine	Sand coarse	CDW
Moisture [%]	10,38	0,07	11,54	2,23	21,87

Materials were kept in tightly sealed containers which prevented the moisture content from changing during the geopolymer material preparation. Materials were taken to smaller containers while preparing the geopolymer and they were used as is, with no preprocessing.

6.2 3D printable material development methods

Geopolymer material formulated for testing is based on the literature review of previous studies in 3D printed geopolymers seen in Table 3 and first material mixes were based on those recipes. The studies can be considered as directive since no straight correlation is seen in the mixtures and standards have not been established for the development of 3D printable geopolymers. Utilizing the information from reported mixtures and proportions of successful 3D printing in literature is recognized as a starting point for the laboratory testing of a new 3D printable mixture development (Kazemian et al. 2017). First material mixes were made according to suitable material proportions and Al/Si ratios used in the related studies. Suitable mix ratios of the raw materials were also generated with solver function for the Al/Si ratio of 1,3–2,5 as in Table 3. Constraints were set that any material could not be zero.

Material mixes were tested for setting, curing and extruding before the more detailed setting test, buildability test and hardened property testing. Extrusion process was simulated by preparing samples in layers with a syringe and different nozzles. The framework and process flow of material development and preliminary testing is presented in Figure 20. The material testing procedure is based on flow charts presented by Panda & Tan (2018) and Ma et al. (2018b).

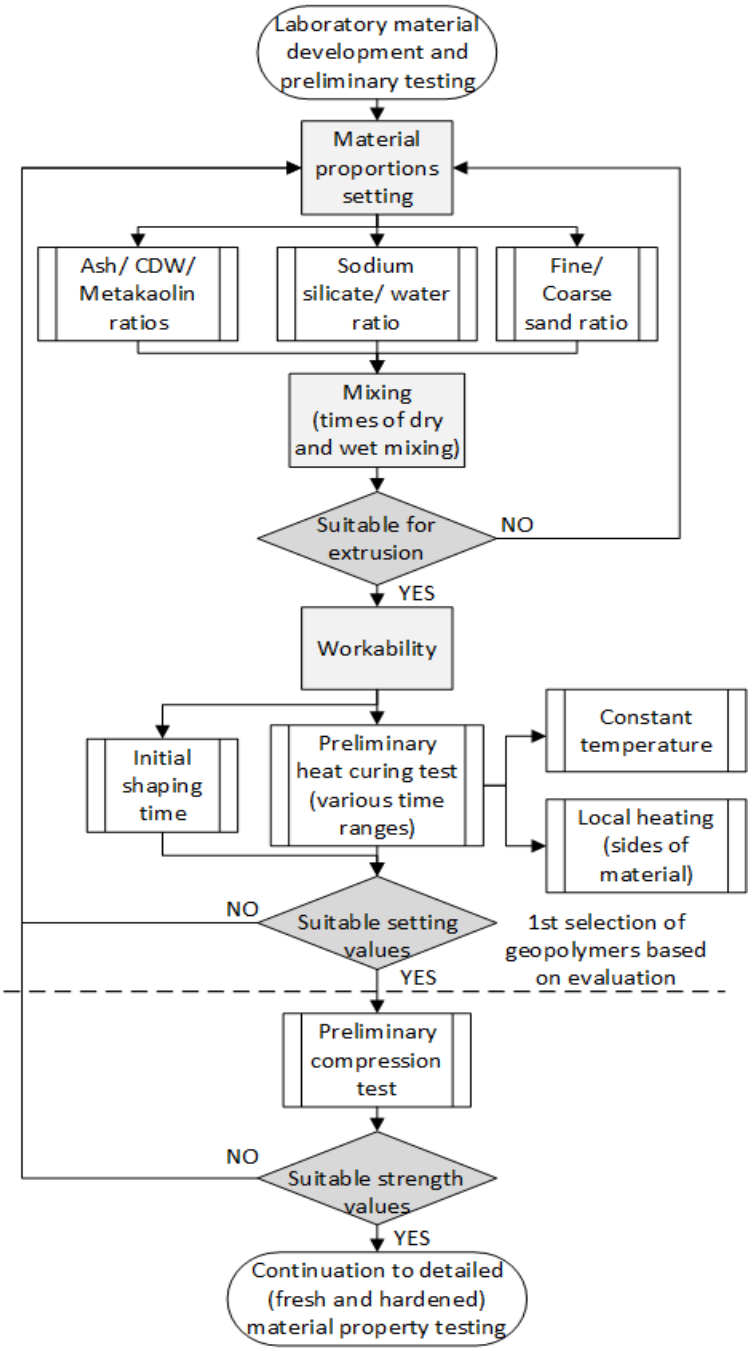

Figure 20. Laboratory experiment process flow chart for material testing of geopolymer for 3D printing.

Before testing of material workability on the detailed level were started, material needed to be workable enough by hand in order it could be poured in molds. Tuning of the material for the following sets was made accordingly based on the behavior of the previous mixture, and process around mixing and mixing proportions revolved until initial workability was established. The effect of each individual component to the behavior of the mixture was evaluated based on its total percentage in the mixture (see results of material development) and decision were made for either adding or subtracting material amount.

Initial shaping times were determined with measuring the time it takes before material could not be shaped in hands without tearing the material. The tests give preliminary values that were used to determine possible open times of the material. Heat experiments were conducted in this stage to determine possible changes in material behavior in means of setting time, flow and open time. Material was heated from top and bottom with air blower and heated plates with temperatures of 60–100 °C. Testing was performed only for materials with shaping times over 5 minutes. The heater used was Steinel HL 2010 E with possible to change the temperature in the range of 50–620 °C. Materials were heated between 10 to 30 seconds to see if crust or skin would start to develop to the material surface.

Every stage was reported, and material was evaluated suitable or not suitable for further testing with criteria presented in the next chapter. Ten geopolymer mixtures with suitable workability and other measured fresh properties continued to further test to determine preliminary compressive strength. Compression specimens for preliminary testing were prepared by casting in 50x50x50 mm cubes and curing them 24 hours in 60 °C oven and then 48 hours in room temperature in order to achieve near maximum strength. Maximum compression in MPa was recorded and material amounts were changed if strength was not satisfactory based on the evaluation.

6.2.1 Evaluation and scoring criteria

Set of criteria were used in order to evaluate the suitability of fresh material properties for 3D printing. Scoring is based on empirical and qualitative evaluation of mixture behavior and early appearance. Scoring was performed for following aspects: behavior in dry and liquid mixing state, mixability of liquid to dry materials, the initial state of mixed material,

a time when material cannot be shaped without fractures, extrudability from different nozzles and appearance after 1-day curing. All aspects are scored scale 0 to 5, 5 being the most suitable. Quantitative values used in scoring were reagent to reactive material ratio, water to reagent ratio, Al to Si ratio and percentage of waste materials. The scoring criteria had different weight factors. Values that had more impact on 3D printing properties and final strength were weight with factor 1,5. Total of ten mixes were selected for strength testing, from which two mixes were selected outside of top ten to verify that scoring criteria were reliable.

Preliminary compression test results were evaluated based directly on the compression strength values. Best performing material mixture was selected for the rest of the material tests. From the most suitable mixture, another version was made with glass wool and continuous glass fibers as additives. Precise scoring criterions are presented in appendix 1.

6.3 Test methods for developed materials

Material testing was performed for fresh state material when the material is still extrudable, and for the hardened state when material had cured for 7 and 28 days. The setting test was used for the determination of open window for the material workability and to give a reference on extrudability. Shape retention test gives values for buildability of material which is an important feature in layer upon layer manufacturing. Hardened properties in compression and flexural testing were carried out to evaluate the performance of the final product. Test methods are classified in Table 8.

Testing was performed for the 2 different materials that were evaluated and found out to be most suitable for 3D printing applications. All materials were prepared in the same way. First ingredients were weighed for the mixture with an accuracy of 0,1 gram. Ash, CDW, metakaolin and sands (and glass wool or carbon fiber) were mixed together for 3 minutes. Next water and sodium silicate were mixed together for 1 minute. Sodium silicate and water were then poured to the dry material mix while constantly mixing. Mixing was continued for 1–2 minutes. Material stuck on sides of mixing bowl were scraped off periodically during the mixing process to attain even mixture. Half of the time was mixed with half speed and rest of time with full speed (400 min^{-1}). Hobart mixer and drill (Makita DHP453) with mixer attachment was used for the mixing process.

Table 8. Test methods for 3D printable geopolymer material testing.

Test	Preparation	Specimens	Amount	Measurements
Temperature setting	Temperatures 20, 40, 60 and 80 °C	Cylindrical container: diameter 54 mm, height 50 mm	3 samples for each temperature (12 total)	13 penetrations (2-minute interval)
Shape stability	Temperatures 20 and 100 °C on sides	Cylindrical container: diameter 54 mm, height 50 mm	3 samples for each temperature (6 total)	5 layer load (2-minute interval)
Compression	7- and 28-day hardened samples (cast and layered)	50x50x50 mm cube (4-minute intervals for layers)	6 samples for each day (3 samples with layer structure)	Samples loaded until fracture (0,9 kN/s)
Flexural	7- and 28-day hardened samples (cast and layered)	150x30x20 mm. (10-minute intervals for layers)	6 samples for each day (3 samples with layer structure)	Samples loaded until fracture (3,55 N/s)

Different time intervals in the test procedures illustrated in Table 8 are based on the planned material application in constructional elements 3D printing. Suitable layering times were set to be around 2 minutes. Times above 2 minutes are used to verify the bonding of the material in case of stops or discontinuity during the 3D printing process.

Specimens for testing are illustrated in Figure 21. For the testing the two different materials total of 102 samples were made. For flexural testing and compressive testing 12 for each material. 3 vibration specimens were included as extra for compressive strength testing made by casting. Extra 3 specimens for flexural testing from both materials were made by making layers in the vertical direction for 28 day curing in order to test layer bond strength. Also, from first material for flexural tests, 6 continuous glass fiber samples were prepared (3 fibers of 2 mm in diameter in parallel and wave patterns) and 3 regular samples that were casted in vibration table. For setting test 12 and for shape stability test 6 specimens were prepared for each material.

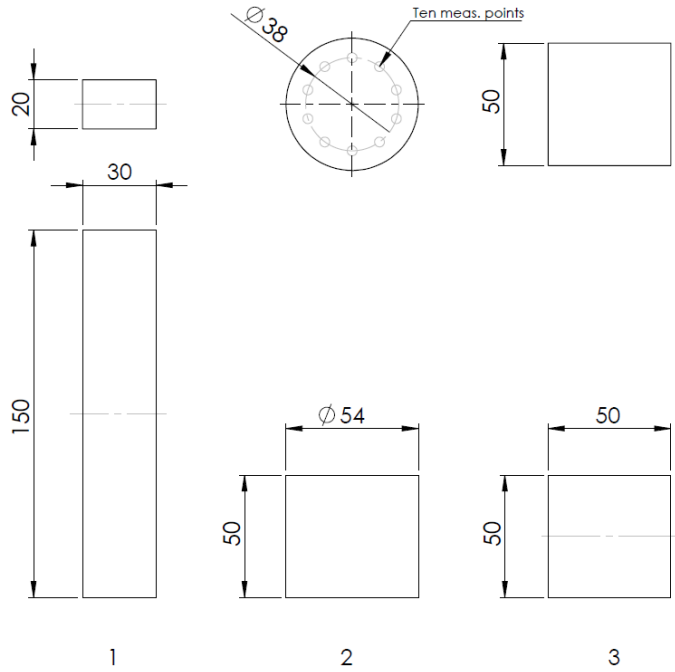

Figure 21. Test specimens for testing: 1. Flexural test, 2. Setting (measurement points illustrated) and shape stability test, 3. Compressive test.

Layers for flexural (vertical layers) and compressive testing specimens were made by extrusion. The interface of the layers is presented with the dotted line in Figure 21. Layering was tested in two different directions with flexural samples. Nozzles used for layering and extrusion tests are presented in Figure 22.

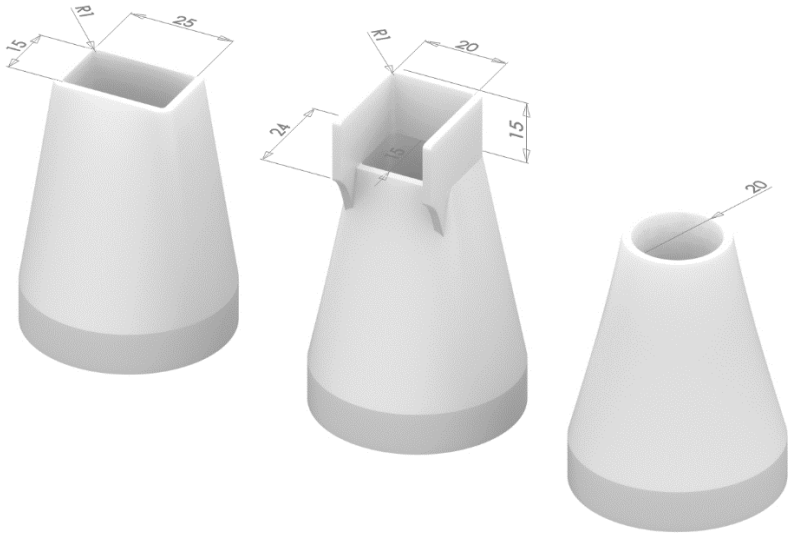

Figure 22. Nozzles used in extruding with orifice dimensions.

All of the nozzles had the same bottom diameter of 43,50 mm from which they were connected to a syringe. The height of the nozzles from bottom to the orifice is 60 mm and uniform thickness of every nozzle is 2 mm. Layering was done with a rectangular opening nozzle on the left shown in Figure 22.

6.3.1 Temperature setting

Temperature setting tests were performed with a specimen size of 54 mm diameter cylinder with 50 mm height. The test is based on a standard test for concrete mixtures time setting according to ASTM C403/C403M-08. Previous standards were used in related studies as described in the chapter 5.1. ASTM standards were used since equivalent ISO standards were not found. Material to be tested were prepared and poured into the specimen mold. Handheld force gauge was used to take the measurements. Round needle with 5 mm diameter on the end of force gauge was penetrated into the material perpendicularly at a constant rate in 25 mm depth. Measurements were taken in 2-minute intervals and penetration forces were recorded accordingly. Up to 13 measurements can be taken from one sample or until penetration resistance exceeds 3,5 MPa. All measurements were done 3 times in all of the temperatures 20, 60, 80 and 100 °C. Heat cabinet was used for measurements in temperatures over 20 °C. The heat cabinet used was Gallenkamp hot box oven size 2. Slight temperature drop took place every time measurement was taken for 30 seconds as the measuring was done outside the oven. Digital force gauge SAUTER FK was used for the penetration force measurements. The force gauge could be used for measurements up to 1000 N with 0,5 N accuracy.

6.3.2 Shape stability

Shape stability (retention) test of fresh material was tested with a cylindrical specimen size of 54 mm in diameter and 50 mm in height (thickness 2 mm). The material was poured into the cylinder which was then removed after a suitable time determined by results from temperature setting test. The change in height was recorded with two Vernier calibers (to 0,1 mm accuracy) from opposite sides of the specimen. The setup used for measuring is illustrated in Figure 23. The material was then loaded from the top with a load equal to a mass of the specimen and change in height were recorded in each step. Total of 5 weight increments corresponding to next layer weight (210 g) were applied on top of the material in 2-minute intervals.

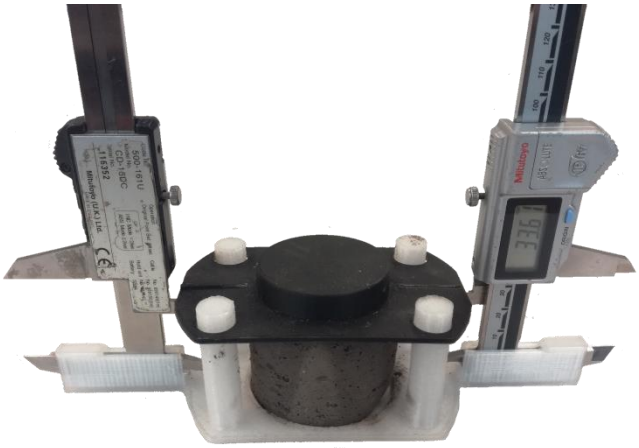

Figure 23. Setup for measuring shape stability. Two digital Vernier calipers are fixed to the platform and the change in height is measured automatically.

To test how heating of sides of layer affects on shape retention, the metal cylinder used for specimen preparation was heated to temperatures 20 and 100 °C. Measurements were made same in each temperature.

6.3.3 Compressive strength

Compression tests were done based on the standard procedure for hardened concrete compressive strength test SFS-EN 12390-3. The material was prepared and poured into 50x50x50 mm molds. Samples were prepared for room temperature curing for 7 and 28 days. Layer effect on compressive strength was tested by making the specimen in two parts: first extruding mold half full and extruding rest of material after a 4-minute time interval. The machine used for compression strength tests was made by ELE International and model was ADR Auto range with a loading rate of 0,9 kN/s for the samples.

6.3.4 Flexural strength

Flexural testing was done with specially made specimens. Size 30x20x150 mm rods were made with a sample mold. Reference samples were made without layers by casting. Specimens for testing of material layer bond strength were made by extruding mixture to bottom half of the mold with a syringe and 25 x 20 mm nozzle. Other half was extruded with a new mixture batch 10 minutes after the first half. Specimens with vertical layers were prepared by pouring the first layer and then 10 minutes later pouring the top half from a fresh batch. Samples were tested after room temperature curing for 7 and 28 days. Specimens were

placed to a testing machine (Zwick/Roell Z020) and loaded with loading rate 3,55 N/s as a center point load. Procedure was done accordingly to SFS-EN 12390-5 annex A.

7 RESULTS OF MATERIAL TESTING

Testing of the developed geopolymers for 3D printing applications were carried out with test procedures described in the methods section. Testing was performed in the same manner for each specimen in each test. Gathered results are presented visually in this chapter with calculated average values and distributions. Measurements were done at least three times for each variation in each test. Average values were calculated and plotted in the same graphs. Error bars are set to illustrate the difference between average value to maximum and minimum recorded values.

7.1 Composition of selected geopolymers

Ten materials were selected for preliminary testing. The naming of the materials was made according to date (letter) and order (number) it was first made. All of the prepared mixtures and their scores are listed in appendix 2. Selection of the materials was based on the evaluation and scoring of each individual material according to the criteria presented in appendix 1. Order of the mixes were set from highest scoring mixture on top and least scoring at bottom. First eight mixtures were also the eight highest scoring mixtures. Material mixtures 4n, 1d and 5p were selected as verification specimens to test the reliability of evaluation criteria. Mixture 4n was used to test the effect of carbon fibers and was otherwise the same as mix 2n. Mixture 1d had higher CDW content and 5p had lower metakaolin content than the rest of the mixtures. Mixtures marked with (*) contains fly ash instead of bark boiler ash. Last column (“min”) is the determined initial shaping time. Compressive tests were carried out for each of mixtures for final evaluation. One specimen was made and tested for each composition.

7.1.1 Final selection of geopolymers

Specimens made for preliminary compression testing were cured in an oven for 24 hours in 60 °C and in room temperature for rest 48 hours before the compression tests. Figure 24 shows the compressive strength values of the mixtures in order from lowest strength to highest. Based on the compression test results 3n was selected for the rest of material and 3D printability properties testing.

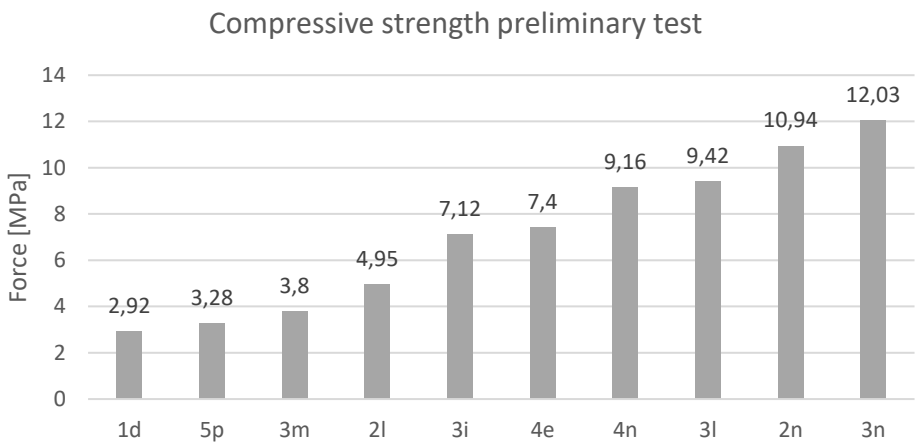

Figure 24. Compression values from initial compressive strength tests.

The second version was made from 3n with 2 percent addition of recycled glass wool to replace the same amount of metakaolin. For the sake of clarity, the geopolymers 3n and 1q are named here on as A and B respectively. The selected geopolymers continued to the detailed testing of setting time, shape stability, compressive and flexural strength. The results of the selected tests are presented in the following chapters.

7.2 Temperature setting results

The material setting was tested with the standard procedure for measuring the initial setting time for concretes. The curve shows the time it takes the material to reach the strength of 3,5 MPa (68,7 N) which is considered as the endpoint for initial setting time. The test was performed in temperatures 20, 40, 60 and 80 °C. In Figure 25 setting development of material A is presented as a line that goes along with the measuring points.

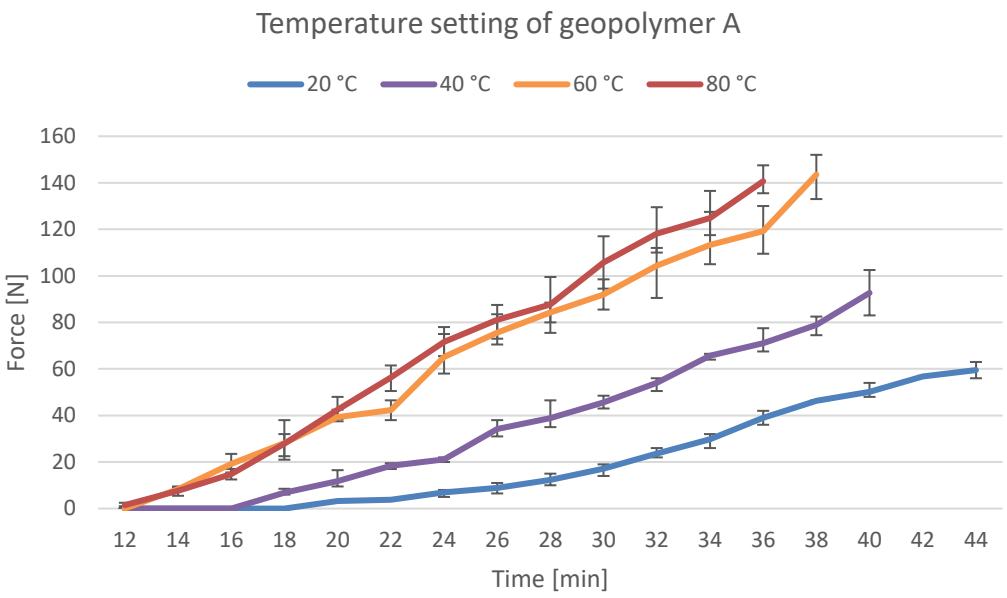

Figure 25. The initial setting time of geopolymer A in different temperatures.

Material A reaches 60 N resistance in 44 minutes at 20 °C, in 33 min at 40 °C, in 23 min at 60 °C and in 22 min at 80 °C. The earliest point when force could be recorded from the samples were at 12 minutes in 80 °C temperature and the latest point was 20 minutes in 20 °C. The temperature setting of geopolymer B is presented in Figure 26.

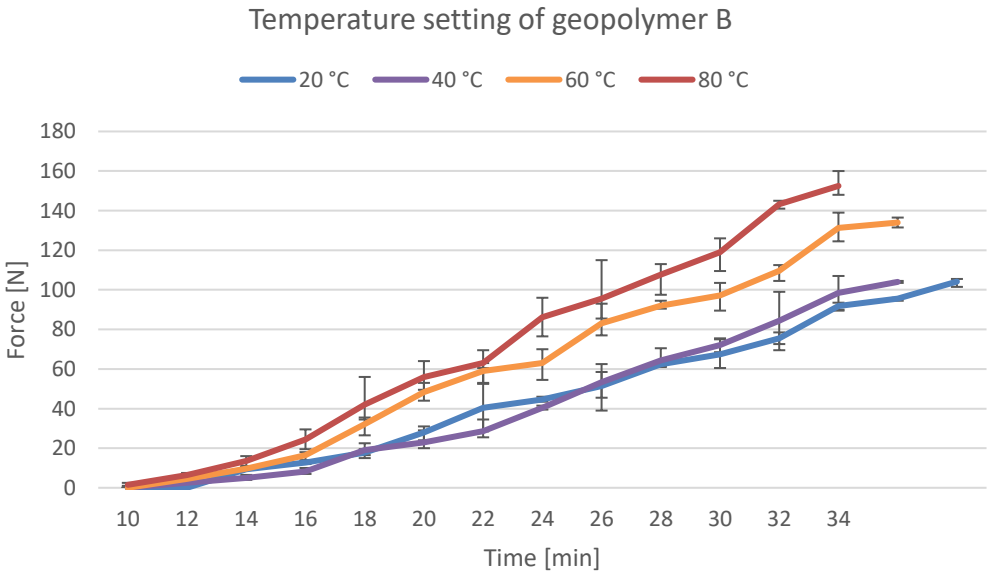

Figure 26. The initial setting time of geopolymer B in different temperatures.

Material B reaches 60 N resistance in 28 minutes at 20 °C and 40 °C, in 22 min at 60 °C and 80 °C. The material started to gain enough strength to be measured at 10 minutes earliest in 80 °C temperature and the latest at 14 minutes in 20 °C.

7.3 Shape stability test results

Shape stability was performed for both A and B in two different temperatures 20 and 100 °C. Geopolymer was poured to the mold straight after mixing. The steel mold was kept in place for 10 minutes for geopolymer A and 6 minutes for B which were half of the time in setting test after force could be measured from the samples. Inside of steel mold was lined with Teflon (PTFE) sheet in order to prevent geopolymer to stick to the mold. The measured deformation (compression) of 50 mm height cylinder from A and B samples are presented in Figure 27.

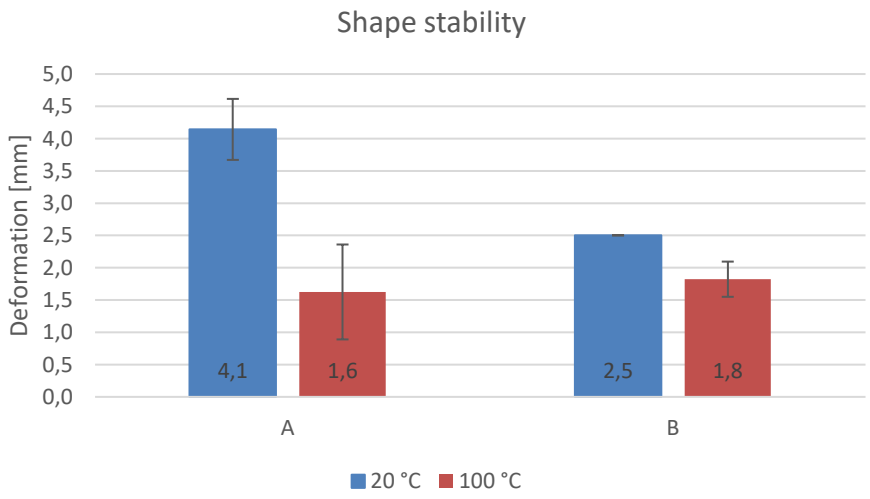

Figure 27. Shape stability of geopolymers A and B in 20 and 100°C.

As seen in Figure 27, the deformation for geopolymer A is 8,2 % from total height in temperature of 20 °C and 3,2% in 100 °C. For geopolymer B the deformations are 5% and 3,6% in temperatures 20 and 100 °C respectively. The deformation of the of both geopolymers during the weight addition is illustrated in Figure 28

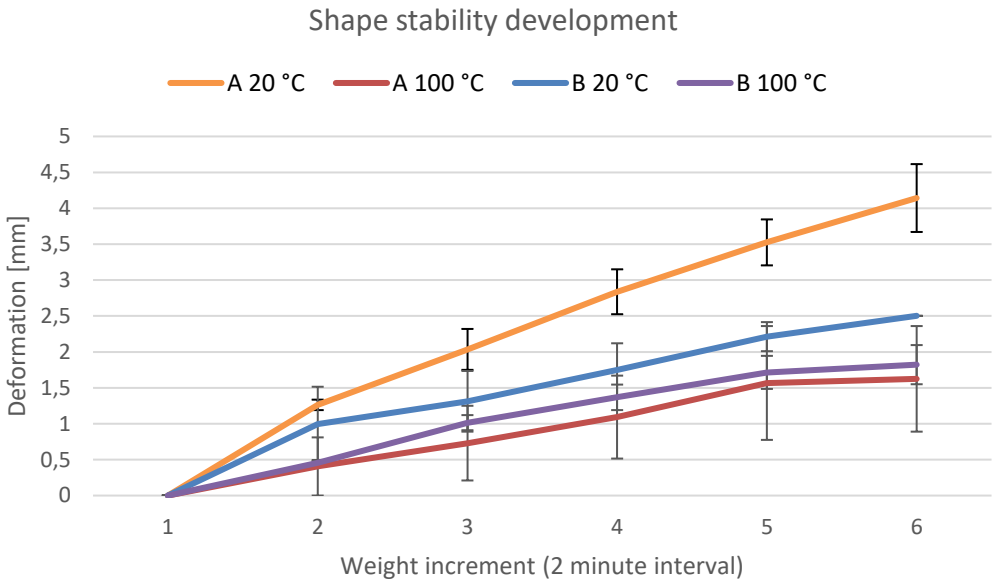

Figure 28. Deformation of geopolymers A and B in 20 and 100 °C.

Total weight on top of geopolymers at the end of test was 10,3 N which equals to around 5,3 kPa. After last weight addition the deformation was insignificant.

7.4 Compression test results

Geopolymers A and B were tested for compressive strength after 7 and 28 days of ambient room temperature curing. The test was made for casted and layered specimens. Results of compression tests are shown in Figure 29.

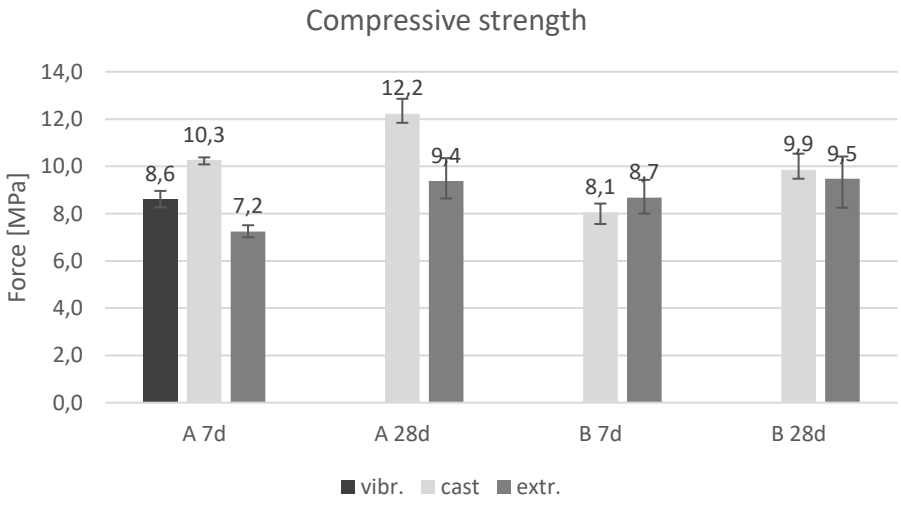

Figure 29. Compression strength of geopolymers A and B after 7 and 28 days of curing.

Quality of compressive test samples shown in Figure 30. Top row illustrates the typical layered samples. Layers were more visible in some samples than others. Top middle and left samples represent 80% of samples (from both A and B) while the quality of the top right sample is seen in rest 20%. In the middle row of the Figure 30 quality of casted samples of B are shown. Sample on right is an anomaly from the rest of casted samples of B that are similar to samples seen in middle and on right. On bottom row casted A samples are presented. Casted quality of A samples were the same for every sample as seen without anomalies.

Figure 30. Examples of compression specimens. On top: extruded B, in middle: casted B and on bottom casted A.

All specimens fractured in the same manner in casted and layered specimens. All four faces exposed during the compression cracked equally which is classified as a satisfactory failure according to SFS-EN 12390-3 (2009). Two tested samples are presented in Figure 31.

Figure 31. Samples after compressive testing. On left, 28 days cured casted A sample. On right 7 days cured extruded B sample.

Sides are still weakly attached to the sample on right in Figure 31, because compression was stopped after the first fractures took place and force was not increasing anymore. Sample on left was compressed longer even after the maximum force was recorded, which caused all sides to detach completely.

7.5 Flexural strength test results

Flexural strength tests were made for casted and layered samples same as with compressive strength test. Three extra test sets were made for geopolymer A for 7-day curing. One extra set was made for both geopolymers A and B for 28-day curing. Flexural strength test results are shown in Figure 32.

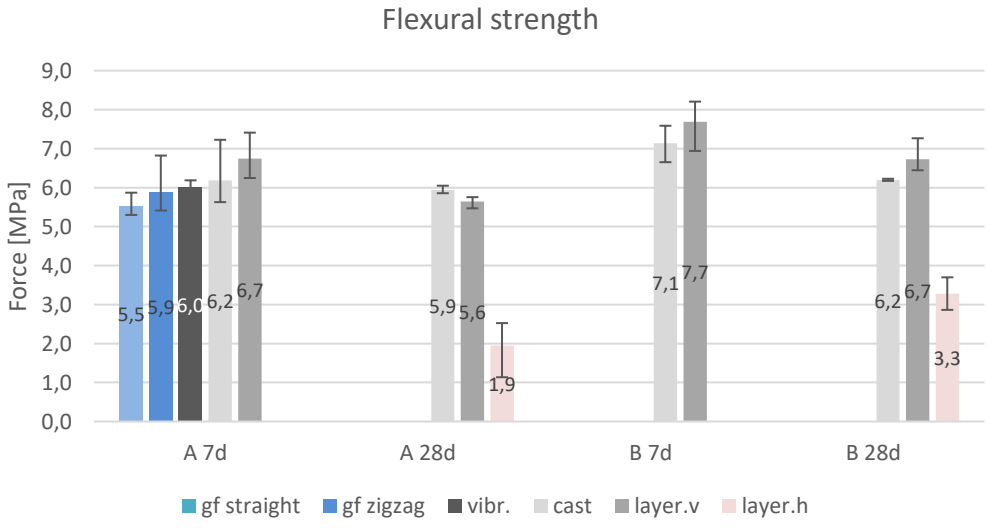

Figure 32. Flexural strength of specimens A and B after 7 and 28 days of curing and their variations.

Examples of flexural specimens viewed from the top and side are shown in Figure 33. All of the specimens with a horizontal layer had a visible layer in the middle. Extrusion caused some uneven surface distributed to the length of extrusion. Few casted specimens of both geopolymers had visible defect cavities as seen in the bottom of Figure 33. Otherwise, all samples had even consistency.

Figure 33. Examples of flexural specimens from top and side view. At top 28 days cured extruded horizontal B and vertical layered A. On the bottom 7 day cured A casted and B.

Extruded specimens with clearly visible horizontal layer line fractured along with the layer interface. All of the samples fractured from the point where force was applied by the upper roller. Fractured samples are presented in Figure 34.

Figure 34. Fractured samples after flexural testing from top and side view. At top 7 day cured casted B samples. In the middle 28 day cured extruded horizontal layer B samples. On the bottom 28 day cured vertical layer A samples.

Fracture line of all samples is relatively straight with only a small angle seen in some samples. Anomalies in fracture behavior were not observed.

7.6 Density

The compressive and flexural strength specimens were weight before both 7- and 28-day testing. The density of different samples is presented in Table 9.

Table 9. Approximate density of cured geopolymers.

Sample	A 7day [kg/m^3]	A 28 day [kg/m^3]	B 7day [kg/m^3]	B 28 day [kg/m^3]
Casted	1693	1618	1752	1621
Extruded	1806	1635	1756	1666
Vibrated	1637	-	-	-

Weight was measured to two decimal accuracy in grams and density was calculated by dividing the weight with calculated volume. Shrinkage was considered in the density

calculation as the cross-section of specimens was measured separately. Density measurements and calculation were not conducted according to standards.

8 ANALYSIS AND DISCUSSION

The results from literature and material testing are analyzed and discussed in this chapter. Connections can be found from the compressive testing and flexural testing since they have been mostly used tests for material analysis. 3D printable geopolymers developed in this study compose mostly from materials that have not been used in any other study, which explains many major differences in comparison. Reasons for the different results are discussed but the detailed scientific explanation cannot be given to all at this point without further research.

8.1 Effect of ingredients in material behavior

3D printable geopolymer material development was based on the related studies where 3D printing performance of different geopolymer mixes was studied. Material proportion setting was based on the studies and values presented in Table 10. The behavior of generated mixtures were observed, and material amount and ratios were tuned accordingly for each material. In appendix 2 every material tested is presented in detail.

Table 10. Average material amounts in related studies and difference between highest and lowest value (Kashani & Ngo 2018, Nematollahi et al. 2018, Panda et al. 2018b, Panda & Tan 2018, Panda et al. 2017b, Paul et al. 2018a, Panda et al. 2017a, Panda et al. 2018a, Lim et al. 2018, Al-Qutaifi et al. 2018, Ma et al. 2019).

[%]	Ash	Slag	Sil.fume	Reag.	Add.	Sand	Si/Al
Tot.	30	6	4	17	1	49	2
Var.	46,8–22,9	15,6–1,5	7,8–1,6	29,8–13,1	0,2–0,9	39,7–54,8	1,5–2,5

Mixtures with over 10% of bark boiler ash showed fast, under 5 minutes setting times. The ash consumed and bound the liquids before all of the material could be mixed, resulting in separate clumps and unmixed dry materials. Also, with high ash amounts, there was a need for raised liquid amounts, especially water and over 1:1 water to reagent ratio in order that material could be mixable and workable. From preliminary compression test results, it was seen that the ash alone does not react well with sodium silicate.

Used ash amount in related studies (Table 10) were on average 23% higher as it worked as primary binder ingredient, than best-performing mixes obtained in this study which had 7% ash amount. The ash type used in this study was completely different than in other studies which use consistently fly ash. The difference in fly ash and bark boiler ash is seen in Al and Si contents. Fly ash in related studies had Al to Si ratio of 2 when in bark boiler ash the same ratio is between 1 to 0,9 This difference was compensated with the use of metakaolin and CDW. Fly ash was also tested in this study, but the production of the used ash was set to be discontinued in early future which made further testing not sensible.

The use of CDW in 3D printable geopolymer formulation has not been discussed in other related studies. The role of CDW was part as filler and part as reactive material due to Al to Si ratio between 2,8 to 4,3. Due to the mixed nature of CDW, the amount of Al and Si can vary greatly (8,5–32,2%) depending on the batch and could be considered more as a filler. Tests with only CDW and sodium silicate resulted in material that crumbled in hands. High CDW amounts (over 27%) had poor strength properties as seen with preliminary compressive tests and scoring of mixes (appendix 2). CDW used in the study were sieved to include max. 4 mm particles biggest particles being rock, soil and styrofoam particles. Styrofoam spheres were part of CDW which worked negatively as voids and cavities in hardened geopolymer mixes and could cause lower strength properties. Overall the suitable amount of CDW in geopolymer mixes was set to be 10% which worked best as partly aluminosilicate source and partly as a substitute for sand fillers.

Sand used in this study were left over product from mine tailings. Sands (coarse and fine) used had no reactive components in them and they worked as a filler material. Geopolymer mixes prepared without sand or low sand levels (under 20%) required more liquids and high (over 1:1) water to silicate ratios since the sand had to be substituted with reactive materials of ash, CDW or metakaolin. Percentage of sands in most suitable mixes were 39% and the ratio between the fine to coarse was between 3,3 and 2. The mixing ratios between fine and coarse sand were found to be not critical when it came to the behavior and strength properties of the geopolymers. Moisture content in the sands caused them to clump and occasionally larger (2 mm) diameter undissolved clumps were left inside hardened geopolymers, which could be avoided by drying the sands before the use and mixing. Sand amounts used in related studies were on average at 49% (Table 10) of the total material amount. The sand

amount at highest was 10% lower in this study due to the nature of the binder materials and the increased need for sodium silicate.

Commercial metakaolin had the highest amount of Al and Si in a total of around 47% with the ratio of 1,2. Metakaolin was mixed together with other dry materials, but also mixing first with sodium silicate and water was tried. Mixing metakaolin alone to liquids left some undissolved metakaolin behind. No difference in material behavior was noted comparing the two different mixing methods. Geopolymer mixes were prepared with different metakaolin amounts and 13% was found out to be most suitable so far when other reactive material (ash and CDW) amounts were 20% or under. Strength properties were lower when metakaolin amount was dropped or other reactive material amounts raised, even if the metakaolin amount was kept at 13%. Found studies on 3D printable geopolymers have not used metakaolin as a precursor, even though metakaolin is used in geopolymer formulation in other fields of geopolymer study.

Sodium silicate with a molar ratio of 2,4–2,6 was used as a reagent throughout this study. In first geopolymer mixes that were tried the reagent and water level were set on the same level as on average (17%) in related studies seen in Table 10. Materials did not mix well with liquid content set below 20% and most well-behaving mixes had a total liquid amount between 28–31%. Water was added to the sodium silicate in order to lower viscosity and enhance workability as done also by Panda et al. (2018b, 2017b) and Paul et al. (2018a). Different water to reagent ratios were tested and the ratio between 3,7–4,2 worked best for suitable strength and workability properties. Lower ratios (under 1) where water amount was higher showed good workability and 3D printing properties, but strength properties were lowered as also described in the study of Ma et al. (2018b).

Additives of glass wool and carbon fiber were tested in strength properties point of view. Glass wool could be added maximum of 4%, amounts over that could not be mixed due to increased stiffness. Glass wool addition caused mixes to set faster with better workability, but slightly worse extrudability and less adherence to metallic surfaces. The change of the geopolymer behavior by adding additives has been recognized by other studies. Use of additives has been carried out in related studies to obtain lower slump with cellulose and actigel addition or better pumpability by adding bentonite (Panda et al. 2017b, Paul et al.

2018a). Chopped glass fibers and different polymer fiber have been used to improve flexural and bond strength of 3D printable geopolymers. Over 1% addition of additives can cause clogging and other problems in extrudability (Panda et al. 2017a, Nematollahi et al. 2018). Clogging and difficulty with workability were most clearly seen in this study with the addition of carbon fiber which made further testing of the material not feasible. Also, continuous glass fiber strings were tested in flexural samples and their addition did not change the material behavior since they were not mixed but instead placed to the mixture during the extruding phase.

Together bark boiler ash, CDW and metakaolin were working as a binder compared to typical 3D printable mixes where the binder consists of fly ash, slag and silica fume. Best performing mixes had binder percentage of 30–33% which was on average 8–5% lower (Table 10) than in related studies. Also, ash was the most used binder material compared to this study where metakaolin was the primary binder. This was due to the difference of the materials and their 11–13% higher need for sodium silicate and water solution. Al to Si ratio of the best performing geopolymer mixtures was around 1,5 when in related studies (Table 10) the average ratio is 2. The Al to Si ratio mostly affects the setting time and hardened properties.

8.2 Comparison of material properties

Fresh and hardened 3D printable geopolymer material properties have been studied by several authors. Setting time, open time and shape stability (buildability) are discussed in the fresh material side. Compressive, flexural and bond strength testing of 3D printable geopolymer has been the main interest in hardened property testing. Comparison between the result of this study and related studies by other authors is made. Differences are analyzed and discussed as they appear.

8.2.1 Fresh material properties

Since setting time have standards in regular concrete preparation, they have been used to test 3D printable geopolymer and concrete setting. Setting time is used to evaluate and analyze the potential open time for material extrusion. At the point when initial setting time is reached material is hardened beyond workability. Basically, the point in which first readings can be measured either with Vicat or penetration test is the start of the initial setting and also

the end of open time. Setting time is directly related to how fast the geopolymerization occurs. Since the differences in materials used in geopolymer formation, the setting times vary in every study depending on the printing purpose. Initial setting times can be usually long as over 100 minutes compared to around 40 minutes in this study. The value does not tell the truth about open time or buildability which must be studied separately.

Open times measured in this study can be described as suitable for 3D printing. Developed geopolymers stay in shapeable state for 10 to 20 minutes. Open times reported in studies of 3D printable geopolymers have varied between 30 to 60 minutes. The open time has been mixed with the setting time in some studies which makes relevant comparison difficult. The main interest in the case of open time is its scaling without affecting final strength and fresh properties in buildability. Geopolymers for 3D printing are either developed for the specific purpose or after material development and determination of open time, printing parameters are set precisely for the object to be printed. In most cases over 10-minute open times are needed due to the size of printed component and speed limitations of used machines. Real open time can be measured by extruding material from a nozzle of wanted size until a blockage occurs. Open time for 3D printing is somewhere between the time after mixing to the blockage since the material can have too low viscosity straight after mixing and too high viscosity long before blockage. The open time is therefore dependent on the material, but also from the equipment used. For example, nozzle size and pumping can increase or decrease the open time, which must be chosen according to the open time that is required depending on the application.

Shape stability for the determination of material buildability has been studied with standard slump tests or methods developed specifically for 3D printable material testing. Usually, the geopolymer is tested straight after mixing, and deformation of 2–6% has been measured (Al-Qutaifi et al. 2018, Paul et al 2018a). Similar deformation values were obtained in this study, but only after 10 minutes of setting and applying heat to the material sides. In an optimal scenario, the deformation should be zero, which can be required for building projects of high standard. Temperature decreases the deformation as will be discussed in the next chapter, but more needs to be done in order to stop deformation completely. Keeping the geopolymer mass longer in a buffer after mixing and applying more heat to the mass before and after extrusion can decrease the deformation even further. The water level in geopolymer mixture

could be lowered for better buildability, which is a compromise with the setting time and could result in the requirement of faster printing speeds and higher pumping pressures. For further buildability testing, real printing setup is needed, since simulation with weight increments cannot tell the real deformation completely. Parameters for obtaining zero deformation in the material during printing should be tested with preliminary printing tests, before changing to full scale.

Results of open time, setting time and buildability in this study suggest that the developed geopolymers are best to be printed over 10 minutes after mixing without applying heat. Buildability is increased as the material can set longer before extrusion. Layering interval can be up to 10 minutes as tested with flexural samples. Material bonds well to the previous layers without affecting the strength properties significantly even after the 10-minute period. With the developed materials the extrusion limit is around 20 minutes after mixing. Open time for the developed materials is around 8–10 minutes starting after 10 minutes from the mixing.

8.2.2 Hardened material properties

Hardened property testing has been the main interest in many studies. Comparison of values measured with the same or similar standards can be made in compressive and flexural results. Every author has concentrated on studying one or two material properties between changing duration which makes comprehensive comparison difficult. In Table 11 results from related studies are gathered and divided between the test samples, preparation method and curing days.

Table 11. Values of compressive, flexural and bond strength of casted and 3D printed specimens after 7- and 28-day curing. (1: Kashani & Ngo 2018, 2: Nematollahi et al. 2018, 3: Panda et al. 2018b, 4: Panda et al. 2017b, 5: Paul et al. 2018a, 6: Panda et al. 2017a, 7: Panda et al. 2018a).

Reference:		1	2	3	4		5		6	7
Curing days:		21	28	28	7	28	7	28	28	28
Comp.	Cast.	58		36	22	35	22	36		
	Print.				21	34	22	36	24	

Table 11 continues. Values of compressive, flexural and bond strength of casted and 3D printed specimens after 7- and 28-day curing. (1: Kashani & Ngo 2018, 2: Nematollahi et al. 2018, 3: Panda et al. 2018b, 4: Panda et al. 2017b, 5: Paul et al. 2018a, 6: Panda et al. 2017a, 7: Panda et al. 2018a).

Reference:		1	2	3	4		5		6	7
Curing days:		21	28	28	7	28	7	28	28	28
Flex.	Cast.			5,1		7,8	6	8,6		
	Print.		7,7			9,5	6,4	9,2	4,2	
Bond.	Print.		3	0,5		0,6			0,7	0,8

In compressive testing 50 mm or 40 mm cubic samples have been used. Casted samples are prepared in a mold with corresponding measurements and printed samples have been extracted from a bigger slab. (Kashani & Ngo 2018, Panda et al. 2017b, Paul et al. 2018a, Panda et al. 2017a) As described in earlier chapters, the composition of geopolymers of the related studies has been different in the composition of the raw materials. Compressive strength is usually measured from different directions of the samples. In Table 11 only compressive strength values measured in parallel to the printed layers are included, as it was the test method used in this study.

As seen from Table 11 compressive strength in both casted and printed samples are higher than obtained in this study during 7- and 28-day curing periods. On average casted geopolymer samples from other studies have 185% higher strength (34,83 MPa) than strength values recorded in this research (12,2 MPa). Printed samples have had a small decrease in strength (2,8 to 4,5%) compared to casted counterparts, while the decrease of strength in this study was more significant for geopolymer A (23 to 30%). An exception is seen with geopolymer B where extruded 7 days cured samples had 7 % increase in strength compared to casted samples, but in 28-day samples, the decrease was similar (4%) as in related studies. The curing time between 7 and 28 days have increased the compressive strength on average 62–63%. The strength of geopolymers A and B increased during the same time period 30,6 and 9,2% respectively in extruded specimens. It is recognized that the time it takes from different geopolymers to go through the geopolymerization process is highly dependent on the raw materials (Duxson et al. 2007). In the case of this study, the materials gain near to maximum strength during the 7 days and the increase is not significant after that.

Fiber additives have been described to decrease the compressive strength since fibers or similar additives that are parallel to the compressive loading can act as voids in the geopolymer matrix (Panda et al. 2017a). The previous phenomenon could explain the lower compressive strength of geopolymer B compared to A, even though glass wool was used instead of fibers. Vibration was tested for geopolymer A to compare it with other 7-day samples. Casted samples that were vibrated showed 16,5% lower strength than conventionally casted samples. Vibration should compact the geopolymer paste more than just plain casting (Nematollahi et al. 2018). The density of vibrated samples was still 1,5% lower than in casted samples. The porosity that was noticeable in every casted and extruded specimen remained even after vibrating the fresh paste. This could be due to chemical processes that happen during geopolymerization, which includes water evaporation.

Flexural strength testing has been conducted almost as much as compressive strength testing as seen in Table 11. The flexural strength values measured in this study are closer to the results from other studies. Mainly 28 days cured samples have been tested by other authors. In casted samples, geopolymer A is on average 18% and B 14% weaker than values presented in Table 11. Casted and 7 days cured samples showed more strength to 28 day cured counterparts. The same behavior has not been reported in other studies. Printed samples show higher strength in this study and in studies by other authors compared to casted samples, opposite to what was observed in compressive strength. No explanation for the previously mentioned phenomenon has been given by any author. Flexural samples with the vertical layers can increase the strength by around 8% found in this study, while the increase in other studies has been 7 to 22%. The only exception of lower strength in the layered sample was observed in 28 days cured A samples. The decrease of layered and casted sample strength between 7 to 28-day samples was 13 to 16% in layered samples and 5 to 13% in cured samples

Porosity, lower density and strength was seen in flexural samples same as with compression samples. As with casted and vibrated compression samples, the vibration had no positive effect on the flexural strength. Vibrated sample had 3% decreased flexural strength compared to casted and 10% compared to vertically layered samples. Opposite to compressive strength, fiber additives has increased the flexural strength, which can be

explained by fibers forming bridges through the cracks that form during application of the force and hence contribute to the flexural strength (Nematollahi et al. 2018, Panda et al. 2017a). Increase of the flexural strength is dependent of the fiber type (3, 6 or 8 mm length) and an increase of 17 to 34% has been reported (Nematollahi et al. 2018). In this study increase of 15% in flexural strength was recorded between geopolymer A and B, even though glass wool was used instead of fibers. Continuous glass fiber samples were included in geopolymer A casted samples for 7 days of curing. Other studies related to 3D printing of geopolymers have described the use of continuous steel fibers as a reinforcement which have formed a mechanical bond with the geopolymer and increased the flexural strength of samples (Ma et al. 2019, Lim et al. 2018). Flexural strength of glass fiber samples had 2 to 8% lower strength to plain geopolymer A. It was clear that there was no mechanical or chemical joining of fibers to the geopolymer, since the fibers could be pulled out almost completely after samples were tested. Higher variation of wave (zigzag) patterned glass fiber samples can be due to the pattern which can result in a situation where only single fiber is under the load directly.

Layer bond strength has been mainly studied with pull off method, where 3D printed sample with 2 layers is glued from both sides to metallic jig plates which are then fixed to a tensile test machine (Panda et al. 2018b, Panda et al. 2017a, Nematollahi et al. 2018). In this study, the bonding strength of the geopolymers was estimated with flexural test setup and samples which had a horizontal layer in the middle. Load was applied directly to the point of the layer interface. In Table 11 bonding strength from different studies is presented with 15-minute layer interval and 28-day curing time. In this study 10-minute interval was used due to the fast setting mixture which makes the comparison only directive. Glass wool additive in geopolymer B makes the bonding increase 74% compared to A and the strength is also 10 to 408% higher compared to the related studies. Results should be confirmed with the same test setup before further conclusions can be made.

Density of the developed geopolymers was considerably low compared to 3D printable geopolymers from other studies. Printed geopolymer densities have been reported to be 2050 and 2250 kg/m^3, while density in casted samples has been lower at 1900 and 2150 kg/m^3 respectively (Panda et al. 2018b, Panda et al. 2017b). The reported values have been measured after 28 days of curing and how the density changes over time were not described.

Casted A and B samples in this study decreased in density by 4 and 7% from 7 to 28 days. The decrease of the density of extruded samples were 9 and 5% for the A and B geopolymers. The density of extruded samples after 28 days curing compared to casted samples was 1 and 3% higher. In related studies, the increase in density was 8 to 5% between extruded and casted samples. Vibration unexpectedly did not increase the density, but instead, the density was decreased by 3%. The density on average was 25% less in 28 days cured samples compared to other studies. The lower density can correspond directly to the lower strength values that were seen in property tests.

Main differences for strength properties of the geopolymers made in this study compared to others is clearly the used materials. As discussed in the material behavior chapter, the Al and Si amounts and ratios were lower in the material used for the geopolymer formulation. The materials may lack some other vital properties for geopolymer formation as materials were not analyzed comprehensively. The difference in used reagents could also explain the weaker strength. Many studies use a mix of sodium or potassium silicate and hydroxide. Hydroxides are corrosive and their use requires extensive protection, which can pose difficulties in large scale printing. The use of hydroxides was avoided for that reason, but with the current precursors, there might not be another way to increase the strength properties if other additives are not used. Flexural strength samples were closer in strength to the typical printed geopolymer than compressive strength samples. As high variation between the flexural strength and compressive strength was not presented in any other study. Also, the decreasing strength in flexural samples over time is a phenomenon that has not been seen in related studies. The geopolymerization process can be the key to the observed behavior and differences. The porosity seen in samples lowers strength and water evaporation can decrease the strength further. In flexural test samples, the pores seem to initiate fracture more easily after curing, which could suggest that porosity and voids have been increased over time. Fractured surfaces should be studied with an electron microscope for further conclusions.

8.3 Effect of raised temperatures

The effect of different temperatures was tested for the behavior of geopolymers mixed during the development phase and after the two most suitable mixes A and B were selected. Similar to all mixtures that were tested on heated plates were that they got stuck to the steel plate

even at room (20 °C) temperatures. Raised temperatures (40–180 °C) that were tested made the material adhere more to the steel surface. Over 100 °C temperatures caused the geopolymers to form a crust of maximum 2 mm in depth from the surface. Below 100 °C made the crust form between depths of 0–1 mm. Heat blower made a skin to form on the geopolymer which thickness was immeasurable. Even though the tested geopolymers adhered to steel surfaces at fresh state, after curing, the material could be removed from the metallic surface in one piece. Curing time takes hours which makes such long contact impossible in 3D printing applications. Studies of locally heating of 3D printable geopolymers were not found which makes a comparison to other studies impossible. Direct physical contact with heated elements should be avoided and heat should be transferred by heat blowers or means of radiation without contact if repellent surfaces are not used. Materials that conduct heat but does not adhere to the geopolymer mixes A and B should be studied further. Teflon coating prevented some of the adhering but not completely.

Curing of compressive strength test specimens were performed by oven curing in preliminary tests. Curing of geopolymers in 60 °C oven for 24 hours and after that in ambient room temperature (20 °C) for 48 hours is reported to result in equivalent strength as 28-day room temperature curing (Nematollahi et al. 2018). Geopolymer A selected for material property testing had 12,02 MPa compressive strength after the oven curing and on average 12,2 MPa strength after 28-day room temperature curing which is in line with other studies. It came clear that heat curing can shorten the curing time by 25 days if the material test is needed to be done in a fast phase without time to wait for a month. In 3D printing applications, heat curing method cannot be considered in most cases if the whole printed object has to be built in heat cabinet, which would limit the size of objects and increase energy costs.

Setting time test with elevated temperatures show clearly that setting time becomes faster. Initial setting time (penetration resistance of 60 N) for geopolymer A was 50% faster at 80 °C and 47 % faster at 60 °C compared to 20 °C. Also, the geopolymer A started to harden 40 % faster in the raised temperatures. The increase rate in setting time slows down radically between temperatures 60 to 80° C where the setting was only 3% faster. The same phenomenon can be seen with geopolymer B. Setting time decreases 21 % between 20 to 80 and 60 °C where the setting time is the same in geopolymer B for both temperatures.

Between the temperatures, geopolymer B begins to harden 28% faster. Between the two geopolymers A and B in the temperature of 60 °C, both geopolymers reach 60 N resistance at the same time (23 minutes). From the timepoint that resistance could be measured the first time it takes geopolymer B 18% longer to gain 60 N resistance compared to geopolymer A. Glass wool addition in geopolymer B makes the material set faster in lower temperatures compared to geopolymer A, but temperature increase does not accelerate the setting as much as for the geopolymer A. Same effect can be seen with the shape stability test.

Temperature setting test revealed that geopolymer B sets faster at room temperatures. This can be seen also with shape stability test where geopolymer B did not deform as much as geopolymer A in 20 °C, where it had 39% less deformation than geopolymer A. In 100 °C the difference in deformation between the geopolymers is decreased to 11%. For geopolymer A the increase in temperature has more impact in shape stability, as also seen with temperature setting test. Deformation drops 61% for geopolymer A and 28% for geopolymer B when the temperature is raised from 20 to 100 °C. Application of heat for better shape stability has been tested by Kazemian et al. (2017b) for 3D printable non-geopolymer concrete. Heat gun with a temperature of 528 °C was used for heating the sides of extruded concrete. Heat application reduced the deformation by 71%. (Kazemian et al. 2017b) Depending on the 3D printing application it must be considered if it is reasonable to use heat for better buildability and faster layering and setting times, or if the addition of additives (in this case glass wool) can perform the same task. The negative impact of glass wool on temperature setting could be due to its insulating property, which then reduces the geopolymerization reaction in the rest of the materials. Delaying the extrusion till the last minute before the material cannot be extruded has usually resulted in zero deformation, but the bond strength between the layers is then compromised.

8.4 3D geopolymer printer structure proposals

Results of the literature review about 3D concrete printers revealed that the basic concept of the 3D printer structures are similar to each other. Biggest differences can be found in printer heads and nozzles in their shape, size and method how they are controlled. Gantry solutions with square, rectangle or round nozzle were found to be most general concrete 3D printer types. Mixing and pumping of the material have been implemented outside of the 3D printer moving parts in 93% of the found solutions (Table 5). Material transportation from the pump

to the nozzle is done with a hose. Pumping the concrete material outside the printer head has been possible due to material properties that are setting after 20 minutes or more from the mixing.

The raw material sources require their own preprocessing which are not discussed but it belongs to the overall process that takes place before the actual 3D printing process can begin. All of the geopolymer 3D printing concepts requires material storage containers, conveyors, mixers and pumps. The most general and simple solution are presented as the traditional concrete printing, where materials are simply mixed, pumped and extruded. For the developed geopolymer two different solutions can be feasible. Proposal one is a solution where all the dry materials and liquids are transported directly to the print head where the mixing and storage would take place. The second proposal is similar to a traditional method with the exception of separate buffer storage near the printer head with heating elements for accelerating the setting process. The print head has side heaters for increased buildability.

The initial concept idea is discussed based on the possibilities found in literature, research and physical testing of the geopolymers. As a concept, the presented ideas, suggestions and values are only directive and simplified. They are still based on real information and data, which justifies the further and deeper investigation of the geopolymer 3D printer development. The sizing of the components is justified with a brief comparison to precast element manufacturing and printer solutions found from literature. When sizing and designing any 3D printer, it is good to keep in mind the Figure 35, which illustrates the unit cost in AM and traditional manufacturing.

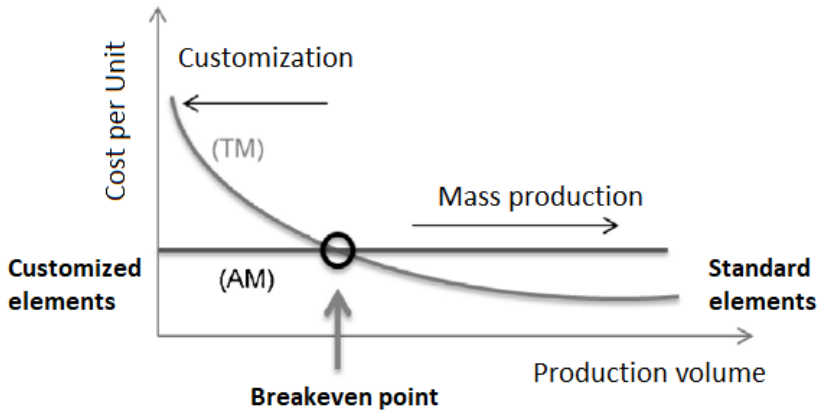

Figure 35. Comparison of unit cost according to production volume in AM and traditional manufacturing (TM) (Mod. Krimi et al. 2017).

It is not reasonable to compare AM of geopolymer or concrete products directly with traditional manufacturing methods in large scale production of the same element. For a large production volume of single elements, traditional manufacturing will always be more efficient. The unit cost of an element from a single printer will always be the same if the same materials and printing parameters are used as seen in Figure 35. The breakeven point is different for every product and depending on the need for a certain product, the point should be calculated, and based on that the choice between printing or traditional methods can be made. The advantage and niche of 3D printing is that it can offer faster production start times for specialized products and lower cost for small production volumes due to reduced formwork and labor costs.

For the developed geopolymer it is reasonable to only print one element at a time, as the setting time and pumping can pose difficulties if several elements are under printing with the same printer setup. Several printers are needed for mass production of elements and the amount and limit on how many printers are feasible to use is determined by the demand for customized construction elements. Typical sizes of precast elements vary depending on the end use. For simple solid precasted walls typical measurements are reported in width: 1,2–4,6 m, height: 3–15 m and thickness: 0,1–0,3 m (PCI 2019). Comparison for precast wall element of size 4x4x0,3 (w, h, t) m is made to give directive values for in which applications and production volumes of 3D printing are feasible alongside with the traditional methods. To justify and determine the size and volume of a single wall element 3D printer, a brief and simplified comparison is made for the production rate of mold precasting.

Estimated building rate in precasting of concrete wall elements is found to be 2,33 m^2/h, which includes formwork, and 1,38 m^2/h in 3D concrete printing. These values are estimations since the rates are case and product sensitive and no universal value exists. In case of 3D printing production, rates are reported to be high as 20,4 m^2/h, but due to differences in printer structure, such configurations could not be utilized for printing designated wall elements. In precast element manufacturing the build rate is usually expressed as m^2/h. The values presented earlier are calculated from the wall of size 3x2,75x0,20 m^3. (Krimi et al. 2017) For the estimation of printer capacity in this study, the

values are compared as m^3/h. Typical build rates in precasting and 3D printing are therefore 0,47 m^3/h and 0,28 m^3/h respectively.

Building rate is calculated separately for the 3D printer component selection in this study since the 3D printers and their capacity presented in the literature vary based on their intended application. The required speed for the 4-meter distance determined by the considered wall width was set to be 2 minutes which equals around 33 mm/sec. Nozzle size of 100x50 mm rectangle is considered for the 3D printer to maximize building rate and adhesion of adjacent layers. With the estimated nozzle size, one layer of the 0,3 m thick wall could be printed with 3 passes. Adjustable side trowels for the nozzle are recommended for better surface quality. Feasible layer thickness for the geopolymer material is estimated to be 50 mm and with that thickness, the 4-meter height wall could be printed in 8 hours (6 minute per layer, a total of 80 layers).

Build rate can be calculated based on the determined application (4x4x0,3 m wall) and calculated speed, which is then used for selection of properly sized components for the concept of a 3D printer. As determined, the layer thickness was set to be 50 mm and width 100 mm, with a printing speed of 33 mm/sec. The previously mentioned values mean that the extrusion rate has to be 0,6 m^3/h (10 liters/min) for successful printing. The build rate sets direct requirements for the size and capacity of the pumps, mixer, containers, conveyors and other required components which are discussed later.

As presented in Figure 35, the customization of the element increases the production cost in the early stage for traditional methods (casting) as in 3D printing the unit cost stays the same. Formwork is reported to be around 53% of the total price in casting when it is made for the first time (Paul et al. 2018a). In Table 12 simplified cost calculation is shown based on the building rates and costs percentages represented in literature. Data of time and cost for 3D printing in construction scale compared to traditional manufacturing is very limited, since 3D printing is a new construction method, which has not been used yet in large scale (Paul et al. 2018b, Yang et al. 2018). The cost composition of the offsite 3D printing can be divided into the cost of 3D printing, manufacturing cost, management fee, profit, transportation cost and VAT. All of the mentioned areas can be divided even further to smaller detailed

fractions. (Yang et al. 2018) Only the five main areas involved with both 3D printing and precasting cost distributions presented in Table 12 are considered and compared.

Table 12. Estimated and calculated cost share and the difference in percentage for typical concrete precast and 3D printing at the start of production and in mass production (Krimi et al. 2017, Paul et al. 2018a, Yang et al. 2018).

Method	Build time	Equipment	Material	Labor	Formwork*	Total cost
Precast	12h	7%	30%	10%	53%	100%
3D printing	8h	+1%	same	-23%	-100%	-54%
The final cost development in mass production (3D printing stays same)						
Precast	9h	-25%	same	-25%	-100%	-57%

*Includes formwork labor

As seen in Table 12, at the start phase of production the cost of the 3D printed element can be 54% less than precasting. Cost of 3D printing is basically fixed, and the price does not decrease even at high volumes as stated earlier. The precasting costs drop after the formwork is done and at the same time build time decreases with equipment and labor costs. If more features are added to the printed elements it would take traditional methods a longer time to reach the breakeven point with 3D printing. As the cost of m^3/h increases in precasting of curved wall compared to the straight wall by 82% according to Krimi et al. (2017), it takes significantly longer to reach the breakeven point with 3D printing, where the cost stays relatively same compared to a straight wall. In the given example (Table 12) the formwork cost and labor are assumed to be dividing equally to the whole production volume in precasting. Only around 100 casted walls have to be manufactured to reach the breakeven point with 3D printing in case of straight walls. As said, the example and values are directive and in real-world applications, the breakeven point can be higher or lower.

8.4.1 3D printer components

With geopolymers formulated in this study, it could be challenging to pump the material distances of several meters without blocking the hose and pipe systems due fast (under 20 minutes) setting times. Mixing and pumping could take place closer to the printhead or at the printhead itself. Only one that kind of solution was found made by Totalkustom for normal non-geopolymer concrete. All the different ingredients need to be transported to the

printhead for final wet mixing, which can pose challenges in pumping and transportation of liquids and dry materials separately. Integrating mixer, pump and possibly other components to the printhead would increase the weight and size, which would require more durability from the printer structure and more power from motors or hydraulics depending on the moving method.

Even with quickly setting mixtures, setting time can be too slow if the material is extruded straight after mixing. Printhead would require mixed material storage or buffer before the printhead where material could set the initial time before extrusion to maximize buildability. With geopolymers tested in this study, it was seen that the setting becomes faster when heat is introduced. Possible heating of the material mixture could be applied in the printhead for the whole mixture before extruding or locally to the material sides to avoid excessive material storage in the printhead. The selected main components are presented in Table 13.

Table 13. Examples of suitable components for geopolymer 3D printer (Scutti 2019, Snyder 2019, Cimbria 2019, M-tec 2019, PCM 2019, Verderflex 2019, Putzmeister 2019).

Component	Information	Details	QTY
Printer	Gantry	10mx10mx5m	1
Containers	Scutti SP 50 (dry materials)	50 m^3	4
	Snyder 13000-gallon cone bottom tank	50 m^3	2
Conveyors	Cimbria Contec SAU200	2 m^3/h	1
Mixers	M-tec D20	20 l/min	2
Pumps	PCM EcoMoineau MVA (for mortar)	0,003–300 m^3/h. 24 bar	1
	Verderflex Rapide R6 (for liquids)	380 l/h max.	2
Buffers	Putzmeister JT 5000	5 m^3 max.	1
Nozzle	100x50 mm opening	Teflon or PP coating	1

Containers are simply for storing the materials before mixing and rest of the 3D printing process is started. A component in the wall example that is intended to print was 4,8 m^3 in volume. Small scale dry cement containers start from 50 m^3 and with that volume, around 10 wall elements could be printed. Own silos are needed for the 4 different materials which mean that the printing amount of around 200 m^3 could be possible before refilling of the silos. With the printer speed, the filling would take place every two weeks if the printer could

operate close to 24 hours a day. There could be a possibility for mixing the two different sands with CDW depending on the preprocessing phase of the raw materials. The selected silo for the purpose is Scutti SP 50 modular waterproof steel silo capacity of 50 m^3 (Scutti 2019). Sodium silicate requires its own separate tank which cannot be the same as dry material silos. Size of around 50 000 liters is chosen since the liquid amount needed for geopolymer preparation is 31% from the whole mass. With the mentioned liter amount, 33 walls can be printed. Tanks are made of high-density linear polyethylene or cross-linked, high-density polyethylene (Snyder 2019).

Material from the silos needs to be transported to the mixer with conveyors. Examples or discussion on the use of conveyors was not found on literature since the scale of printers has been small with no conveyor required. Conveyor without detailed description is seen in the presentation of Leal de Silva (2017). Geopolymer mixing plant manufacturer Renca (2018) has utilized solution with screw conveyors for transporting geopolymer binder to the mixer. Screw conveyor Cimbria Contec SAU200 with a capacity of 2 m^3/h according to Cimbria (2019) is selected, which fulfills the minimum requirement of 0,6 m^3/h. Possibility for geopolymer premix in one silo could be considered, which could eliminate the need for conveyor if the mixer is placed straight under the mixer.

Choice of the mixer is based on material properties of the developed geopolymer. The sticky nature of the material can create challenges for the mixing of the material. Mixer with continuous loading can create issues with material covering the mixer blades with time as experienced in mixing of the developed geopolymers. Regular wash and emptying of the mixer during printing of several hour prints can be inevitable. Two mixers can be added for reliability and to ensure continuous mixing while another mixer is under cleaning. Continuous mixing can be utilized with mixer capable of mixing rate of 10 l/min as calculated earlier. Selected mixer M-tec D20 is developed for mortars with particle sizes under 4 mm (M-tec 2019). The developed geopolymers in this study resemble mortar which makes the chosen mixer suitable for the purpose.

A most suitable pump for the pumping of the geopolymer developed and tested in this study would be a progressive cavity pump. Progressive cavity pump offers the most constant flow compared to other found solutions of peristaltic pump and screw pump. Piston pumps can

also offer better constant flows but the sizing of pistons to hold the amount of geopolymer that can be extruded before initial setting time in all size of 3D printing objects can be challenging. Sizing of the selected pump is made according to the required printing speed and material deposition rate. The calculated material deposition rate for the example case should be around 0,6 m^3/h as presented earlier. The flow and pressure rate in progressive cavity pumps can be controlled in a wide range. The selected pump is PCM EcoMoineau MVA that is also suitable for pasty and sticky materials according to PCM (2019), which makes it suitable for the developed geopolymer. Separate pumps are needed for reagent and water supply. Peristaltic pumps were found to be suitable for pumping liquids. With the required build rate, liquids need to be pumped at a rate around 190 l/h as the composition of developed geopolymers contain 31% of liquids. Example of a suitable pump is Verderflex Rapide R6 with 380 l/h maximum pumping rate (Verderflex 2019).

Since the geopolymer is too viscous after mixing to be pumped straight to the nozzle a buffer is needed where material can rest initial time (around 10 minutes) to gain better buildability. Rotating buffers are seen mostly in concrete trucks that keep the concrete flowing during transport to the construction site. Buffers are not usually needed in mold casting or 3D printing applications which makes the selection and supply of concrete buffer storages limited. Putzmeister offers concrete reservoir buffer with a capacity of 5 m^3 (Putzmeister 2019). The size for the designed application could be too large and the possibility to design and manufacture own buffer in more suitable scale should be considered.

The nozzle has been commonly manufactured from steel materials, apart from laboratory scale printers where examples of plastic nozzles were found. Nozzle for the case example application in this study could be made directly from 100x50 hollow rectangular steel element with thickness around 3 mm. Separate side trowels with heating possibility should be integrated into the nozzle as the experiments revealed that heating increases the buildability of developed geopolymers. The sticky nature of geopolymers due to the alkaline reagent can cause problems in extruding phase if the material adheres to the nozzle sides. Steel can be lined with Teflon, as tested by Wolfs et al. (2018). Another material suitable for steel nozzles to prevent adhering with concrete is polypropylene (Lloret et al. 2015). Teflon coating was tested in the experimental phase of this study and it turned out to be suitable for the application, and it is recommended for full-scale use. For heating the nozzle, metallic

electrical resistance heated elements or heat blowers can be used with the possibility to control temperature with 5 °C accuracy.

Yearly capacity of one geopolymer 3D printer would be 1752 m^3 or 365 walls if the machine is operated 8 hours a day. Due to reduced need for labor, 24-hour operation can be possible to some extent which would mean yearly production of 5256 m^3 and 1095 walls. Regular maintenance is required for the machinery which makes the values only theoretical. Only the main components were presented. The whole assembly would need a design for the connections and other structures in order to make everything work seamlessly. In order that more detailed conclusions or proposals of the structure and features for geopolymer 3D printer can be made for the developed material, preliminary testing of 3D printing with different parameter combinations needs to be conducted.

8.5 Objectivity

The research conducted and presented in this paper belongs to a project with the goal to develop geopolymer material and printer that can be utilized for infrastructural building projects. Results are used for developing material further and to give guidelines for 3D printer machine structure. All sides of the use of geopolymers and 3D printing in infrastructure applications were taken account in results of the literature and material testing, even though the nature of the project is to promote possibilities and advantages of 3D printing of geopolymers made from local industrial side stream materials.

Methods and results are described in detail and standardized methods were used in testing of compressive and flexural strengths. Material testing methods that did not have or did not comply with standards were described and justified with methods utilized in related studies. Main factors and conditions affecting the measurements and material behavior are described as they have occurred. Results and measuring values were described and recorded as precise accuracy as possible. Some of the results show inconsistency which are presented as with all other results and issues with repeatability is acknowledged. Used materials in this study can change over time due to weathering and drying. Also, the materials can change depending on where they are sourced. The previously mentioned factors are difficult to avoid, which can limit the repeatability of the results in this study. The obtained results have a resemblance

to several earlier studies conducted by different authors, which gives the values and methods credibility.

8.6 Reliability, validity and sensitivity analysis

Reliability and validity review in this study focuses on the material development and testing side. Reliability was ensured by mixing the same material multiple times during the experiments. Testing of the properties were conducted with at least 3 times for each material and specimen. A sample size of 3 in every material property testing was relatively low due to resources limitations in some materials availability. Variation was moderate for each set that was tested in compressive and flexural tests as the conditions did not change during the research and measurements intervals. The material was prepared and mixed in the same manner for the entirety of the research and the reliability is seen from the compressive and flexural test results since they do not display anomalies. Reliability in temperature setting and shape stability test could be described to be the same level as in other test methods. The used measuring devices of digital force gauge (accuracy 0,5 N) and digital Vernier caliber (accuracy 0,02 mm) were operated in the same ambient temperature and condition separately from a material that was heated. The variation in measurements is caused by changing material behavior in a fresh state, which should be measured separately before further reliability of used measuring methods can be concluded. Verification measurements could be conducted by repeating some of the tests and using a larger sample size for ensuring the reliability of the presented results. There is still no reason to doubt that with the same materials and methods results could not be replicated somewhere else by other researchers.

The validity of the results can be concluded to be high as the measuring methods were clear and the measuring devices used were meant for the specific purposes. Results are generalizable as there is conformity in the measured values and resemblance to other studies. Printing properties were measured indirectly in this study with different test methods. Measurements were made similarly to related studies of 3D printable concrete which gives them validity. Heating caused the material to set faster, extruded compressive samples had lower strength than casted samples and flexural strength was increased with layering as also seen in studies by other authors. Only differences were observed in strength loss of flexural samples after 28 days of curing. Validity in analysis and interpretation of results could be more advanced. Analysis at this point was based on visual observations and numerical values

of individual material components. The overall composition of developed geopolymers could be studied for more deeper analysis and predictions on material behavior and properties between different tests.

In this research, sensitivity can be described by how changes in the materials from which the geopolymers where prepared would affect the measured values in several test methods. Different ingredients were stored in their own containers tightly to prevent changes in moisture content. While preparing different mixes, the materials were collected to smaller containers and stored in them for maximum time of 24 hours while geopolymer mixes were made. Even though the temporary containers were airtight, some moisture could have evaporated. Changes in moisture content may lead mainly to changes in material mixing and strength properties. Results still show that there is no significant variation in mixed material properties that could be claimed for the moisture content changes. There is no reason to assume that the chemical composition of materials would have changed either. Sensitivity analysis was also utilized in the material development phase. Individual materials were tested in mixes in high and low contents. If obtained fresh behavior and strength values were not suitable, the decision on increasing or decreasing the particular material amount was made accordingly.

8.7 Topics for future research

The 3D printing testing was relatively limited in this research as the material was not actually printed with real 3D printer equipment. Several areas could be researched in the future, in order to determine material behavior more precisely under different circumstances. Further material development and investigations are needed prior to implementation of the material elsewhere. Possible future research topics based on this research are:

- 3D printing the material with the test setup. Testing of different printing parameters in speed, pumping pressure, layer cycle time and nozzle size.
- Testing of different alkaline reagents and their effect on strength and material behavior.
- Conducting more precise tests for hardened samples in compressive, flexural and bond strength with different parameter combinations.
- Testing of different materials that have been used in related studies (slag, silica fume etc.).

- Preprocessing of the recycled materials before preparing geopolymers (sieving Styrofoam out of CDW etc.).

8.8 Summary

The research was guided by the research questions, and answers were sought for them by utilizing literature and physical material testing methods acknowledged by the research community. Areas under interest in this study were: machine setups that are suitable for geopolymer 3D printing, how to develop 3D printable geopolymer from predefined industrial aluminosilicate byproducts, how applying heat affects to fresh geopolymer behavior and how printing parameter and different material mixing rates change strength properties of geopolymers. Conclusions for the previous areas are presented below.

All the machine setups for geopolymer printing contain basically the same components with different scaling, which depends on the end use of the printer. Printing of geopolymers can be also done with the same equipment designed for regular concrete 3D printing. The basic hardware that is included in every concrete (geopolymer or traditional) 3D printer includes at least: material containers (silos), a mixer, a pump and an extrusion nozzle (print head). Method for controlling the print head and material deposition in layers have been done with three main configurations: gantry, robotic arm and crane. Size of the structure is adapted for the component to be printed. Robotic and crane solutions have limitations for the size of the component, while gantry solutions are more scalable. It must be considered that one printer cannot print everything. If the 3D printer is designed for printing houses or structural elements, it is unlikely that under cubic meter size detailed components can be printed credibly, and the same goes also another way around. Even if the 3D printer is scaled properly to print structural elements, reasonability must be considered, since casting and other traditional methods will outperform 3D printing when it comes to mass production. Geopolymer 3D printer machine configuration must be considered from all of the above-mentioned perspectives before the decision of application area, sizing of printer components and type of printer to be used can be made.

The Al to Si ratio of the best performing mixes were 1,5. The best performing mixes had a connection to literature when Al to Si ratio was compared. The mixing rates of the materials only correspond to this study. Waste materials with the same levels of aluminum and silicon

can behave completely different when mixed together if the composition is otherwise dissimilar. The Al/Si ratio can give a clue on which material proportions can work suitably for material development. During experiments, it was found that Al/Si ratios that were suitable in best performing mixes can be achieved with completely different material proportion setting which did not work as well. A suitable material cannot be simply developed by calculating Al/Si ratios, but instead, individual materials need to be experimentally tested and mixed in small amounts in order that conclusions on material behavior can be made.

3D printability is a vast concept and two same 3D printable geopolymer does not exist. Geopolymer or cementitious material that can be extruded after mixing and another layer can be placed on top of it so that they adhere to each other and keep their extruded shape irrelevant of time duration, can be called 3D printable. The object, part or structure to be printed determines the required fresh and hardened material properties. Several printable materials were obtained in this study according to the previous definition. Some materials were printable only for 2 minutes, while others lasted for 30 minutes and had poor strength. The predefined application of 3D printing wall elements set the requirements for acceptable printability, which were obtained by the two geopolymer mixes discussed in this study. Proper 3D printability of the developed geopolymer materials is yet to be tested with 3D printer setup. Tuning of the material mix for better strength properties is still needed before full-scale printing can begin.

Heating was tested for the fresh material properties, which has not been discussed in geopolymer 3D printing related studies. Geopolymers are known for their accelerated curing time in heated temperatures. How heating could be applied to the 3D printing process was unknown. Setting test in elevated temperatures revealed that the setting does not accelerate significantly after 60 °C. Geopolymer mass could be heated in a buffer container after mixing in printing processes where increased buildability is required. Heating of the geopolymer mass results in crust or skin formation on the material surface, which can make working with the material difficult. Keeping the material in constant flow by mixing can help to maintain workability. Final Strength of developed geopolymer material can be gained in a 24-hour heat curing period. In large scale 3D printing applications heat curing cannot be applied to the whole structure as it would be too excessive in energy consumption point of view.

Applying as low heat as possible should be used, since with material design buildability and setting time can be increased for example with the addition of glass wool as seen in this study. The use of accelerators or decelerators could be replaced partially with heating of the printable mass before the extrusion, which would allow broader open window and better pumpability when the material does not have to be as stiff before the extrusion.

In the material development phase, much as possible industrial byproducts were tried to utilize for the 3D printable geopolymer formulation. The main byproducts of ash and CDW showed insufficient printing and strength properties when they were used alone. The amounts of ash and CDW had to be kept under 20% in the total mixture together with 11–13% of metakaolin, in order to achieve the best strength properties. The used sand in this study was also industrial byproduct, but it did not contribute much to the strength of the material as it worked as a filler. Still sand is required suitably over 40% in the mixture in order to achieve maximum strengths.

3D printable properties of the geopolymers were tested with the 25x15 rectangular nozzle. For compressive strength samples, a total of two layers were extruded in the 4-minute interval from the same material batch. Even though the extrusion printing compresses geopolymer and makes it denser compared to casted counterparts, the strength of the extruded samples were lower. Since the layers are parallel to the compression, the same strength as in casted specimens cannot be completely reached. Right kind of nozzle geometry and pumping pressure can still contribute to the strength properties positively, which requires further studies with the developed geopolymers. Casted samples show the ultimate potential that can be achieved in compressive strength with proper printing parameters.

Flexural samples showed possible improvement in strength with layering compared to the casted samples. A fresh batch of geopolymer that was poured on top of the previous layer in 10-minute interval increased the flexural strength. The limit of time when strength properties do not increase anymore in layering should be studied. As seen with the compressive and flexural samples it can be concluded that it is better to print next layer with fresh material batch as better strength properties can be gained compared to the mixture that has been setting longer. This has to be compromised with buildability, which requires material to be setting initial time because material straight after mixing can have too low viscosity for

printing. Mixing of the different materials is always a compromise between strength and printability. Materials that can be printed well did not have sufficient strength and materials that had good strength were not as well printable. Also, it has to be determined what strength properties are most important in the applications. Fiber addition will increase the flexural strength, but in the same time decrease the compressive strength, which can pose difficulties if both are needed to maximize. The balance between printing parameters, materials, additives, heat and strength must be set each time for specific purpose depending on the application and required properties, which will mean that compromises must be made every time in one or two of the mentioned areas.

Without further research on developed material composition, it cannot be objectively stated that the material is in fact geopolymer at all. The line between geopolymers and alkali-activated materials is narrow. The goal of the research was to develop sustainable 3D printable material from industrial side stream byproducts and the precise terminology describing the material was out of scope and further classification should be done when the material is studied further. Geopolymers obtained in this study are suitable to start a real 3D printing test with test equipment. Use of industrial byproducts that otherwise would go to waste or landfill can be viably recycled into 3D printable geopolymers. Tuning needs to be done before full scale can be implemented. Strength properties must be increased, open time and buildability optimized. Several other tests should be conducted before the material can be used in real constructional applications.

9 CONCLUSIONS

Climate change and a growing population require better control and reduction of CO_2 emissions. The task is difficult as the population around the globe is growing in an increasing rate. More housing, accommodation and infra building is needed at the same pace. Production of concrete from OPC is a major source of CO_2 emissions in the world as it is the most used building material. An alternative material for traditional concrete is geopolymer. Geopolymers contain similar materials as OPC concrete and can have the same or better qualities as concrete depending on the composition. Production of the cement used in concretes creates most of the CO_2 emissions. Geopolymers rely on alkali activation of aluminosilicate materials and do not require the use of cement, which makes geopolymers more sustainable. A lot of recycled and waste materials contain aluminum and silicon which makes them suitable for geopolymer preparation. Traditional building and construction methods produce a lot of waste, as the molds that are needed for casting the structures or elements cannot be reused. Less waste is generated with 3D printing compared to traditional concrete working methods, which can promote sustainability even further when used together with geopolymers. Aim and goal of this research were to study and develop 3D printable geopolymer material that utilizes local industrial side stream materials. The end use of printed components was set to be in constructional and infra elements, which was the scope in the testing of material fresh and strength properties. 3D printers were studied in general in order to develop a concept idea of geopolymer printer, with required components and sizing.

A literature review revealed that geopolymers can be prepared from several different materials with aluminosilicate content. Fly ash, slag and silica fume have been the main ingredients in 3D printable geopolymer preparation. Several different factors need to be maintained in material and equipment side during the 3D printing process. Each geopolymer has their own open time window when the material can be extruded after mixing since the material starts to harden straight after mixing process. Main components needed in extrusion 3D printing of geopolymers are a mixer, pump and nozzle. Printer head and the nozzle are typically controlled by the gantry, robotic or crane construction. The setting time and

rheology of the geopolymer material sets specific requirements for the components to be selected to ensure sufficient mixing rates, pumping pressures and extrusion speed.

Several testing methods are used for determining fresh and hardened properties of printable geopolymers. In fresh material testing side, setting time and shape stability test have been most commonly used. Setting time test measures the rate of material hardening and shape stability describes how the material behaves under a load of subsequent layers. Hardened material properties can be tested with a standardized test method developed for concretes. Common tests applied in 3D printed geopolymer testing have been compressive, flexural and bonding strength tests.

Materials used in this study to develop 3D printable geopolymer differed from the literature as recyclable material use in printable geopolymer development had not been conducted. Boiler bark ash, CDW, metakaolin and mine tailings were mixed together with sodium silicate and water. A systematic approach to material development and testing was applied. Evaluation and scoring of different mixes and their iterations based on qualitative and quantitative values resulted in two geopolymer materials that were selected for further testing. Application of heat was tested in setting and shape stability testing as heat promotes the curing of geopolymers and lacks research in that field. Testing procedures were done according to standards in hardened material testing and test method from related studies were applied in fresh material testing as found in the literature.

Fresh material properties of the developed geopolymers were found out to be suitable for 3D printing with few prerequisites. Geopolymers had initial setting times of around 38 and 44 minutes which could be accelerated with the heat introduction. Shape stability was gained in 10 to 8 minutes which could be also enhanced with heating the geopolymer between temperatures 40–100 °C. The tested geopolymers cannot be then extruded straight after mixing. The controlled setting can be done in separate buffer with possible heat introduction prior to pumping through extrusion nozzle. Buildability and shape stability are increased also if heat elements are attached to the nozzle with trowels. Results were promising for further development. Printability can be significantly increased with heat and correct material proportions.

Hardened material property testing results showed that strength properties should be enhanced with further material development before utilization of geopolymer can take place on a larger scale. Even the best compressive strength results were 45% lower than the lowest values recorded in related studies. Otherwise material properties behaved as predicted when printing was simulated. Compression in parallel to the extruded layers causes a decrease in strength which is not a good sign for printability. At the moment there is no solution for the problem presented anywhere in geopolymer printing related studies. Decreasing of recyclable materials in the geopolymer mix increased the overall strength when commercial aluminosilicate materials where substituted, but values were still off the target. Flexural strength was closer to values that had been gained with 3D printed geopolymers in other studies and only under 18% lower values where observed. Flexural strength could be increased with additives, unlike in compressive strength. Maximizing other strength values means tradeoff with another. Printing simulation increased the flexural strength, but as with the same time, compressive strength was reduced. The decreasing strength in flexural samples over time opposite to compressive strength would require deeper knowledge in geopolymer formation of the presented materials. Vibration or continuous glass fiber strings could not increase the strength properties of geopolymers which means that alternative solutions should be investigated. The results clearly state that strength properties should be increased, which requires more research on material development. Compromises must be done in many areas in the material strength and printer constructions. Strength and recyclability can be seen as a compromise where increasing the other requires the other to decrease. What compromises can or have to be done depends on the product that is 3D printed and its application area.

Competing with 3D printing against the construction industry is not reasonable. 3D printing could be integrated as one part of the construction markets. Specialized products, complex geometries and small production volumes are areas where 3D printing has an advantage. Production can be started faster with printing when molds are not needed and need for labor is also reduced. Rising demand in sustainable constructional solutions will most likely promote and increase the share of geopolymer 3D printing as the state of technology improves.

Developing 3D printable geopolymer material entirely out of recycled materials or waste products can be challenging. The fact that used materials for geopolymers contain aluminum and silicon alone is not enough for material development. Used ash, CDW and other side products must contain correct ratio of the elements favorable in geopolymerization. Still it can be stated that recyclable products could be utilized in greater amounts in 3D printable materials even as fillers.

LIST OF REFERENCES

Abrams, M. 2014. 3D Printing Houses. [asme webpage]. [Referred 29.10.2018]. Available: https://www.asme.org/engineering-topics/articles/construction-and-building/3d-printing-houses

Al-Qutaifi, S., Nazari, A. & Bagheri, A. 2018. Mechanical properties of layered geopolymer structures applicable in concrete 3D-printing. Construction and Building materials, 176: 2018. Pp. 690–699.

Apis cor. 2017. Technology description. [web document]. [Referred 29.10.2018]. Available in PDF-file: http://apis-cor.com/files/ApisCor_TechnologyDescription_en

ASTM C403/C403M-08. 2008. Standard Test Method for Time of Setting of Concrete Mixtures by Penetration Resistance. Pennsylvania: American Society of Testing and Materials. 7 p.

ASTM C618-12a. 2012. Specification for coal fly ash and raw or calcined natural pozzolan for use in concrete. West Conshohocken: American Society of Testing and Materials. 5 p.

Bos, F., Wolfs, R., Ahmed, Z. & Salet, T. 2016. Additive manufacturing of concrete in construction: potentials and challenges of 3D concrete printing. Virtual and Physical Prototyping, 11: 3. Pp. 209–225.

BMH systems. 2018. Twin shaft mixer. [BMH systems webpage]. [Referred 31.10.2018]. Available: http://www.bmhsystems.com/plants-mixers/mixers-equipment/twin-shaft-mixer

Buswell, R. A., Leal da Silva, W. R., Jones, S. Z. & Dirrenberger, J. 2018. 3D printing using concrete extrusion: A roadmap for research. Cement and Concrete Research, 112: 2018. Pp. 37–49.

Cimbria. 2019. Cimbria Contec screw conveyors. [Cimbria webpage]. [Referred 22.3.2019]. Available: http://www.cimbria.com/products/conveying/screw-conveyors

Constructions 3D. 2018. [Constructions 3D webpage]. [Referred 29.10.2018]. Available: https://www.constructions-3d.com/

Cusack, R. 2018. How technological advances can help meet housing targets. [lgcplus webpage]. Updated May 31, 2018. [Referred 29.10.2018]. Available: https://www.lgcplus.com/services/regeneration-and-planning/how-technological-advances-can-help-meet-housing-targets/7024646.article

Davidovits, J. 2013. Geopolymer cement. [web document]. [Referred 29.10.2018]. Available in PDF-file: https://www.geopolymer.org/fichiers_pdf/GPCement2013.pdf

Delgado Camacho, D., Clayton, P., O'Brien, W. J., Speersad, C., Juenger, M., Ferron, R. & Salamone, S. 2018. Applications of additive manufacturing in the construction industry – A forward-looking review. Automation in Construction, 89: 2018. Pp. 110–119.

DTI. 2018. 3D printed buildings. [DTI webpage]. Updated October 8, 2018. [Referred 29.10.2018]. Available: https://www.dti.dk/projects/3d-printed-buildings/36993

Duxson, P., Fernandez-Jimenez, A., Provis, J. L., Lukey, G. C., Palomo, A. & van Deventer, J. S. J. 2007. Geopolymer technology: the current state of the art. Journal of Materials Science, 42: 9. Pp. 2917–2933.

Ferraris, C. F. 2001. Concrete Mixing Methods and Concrete Mixers: State of the Art. Journal of Research of the National Institute of Standards and Technology, 106: 2. Pp. 391–399.

Ghaffar, S. H., Corker, J. & Fan, M. 2018. Additive manufacturing technology and its implementation in construction as an eco-innovative solution. Automation in Construction, 98: 2018. Pp. 1–11.

Gosselin, C., Duballet, R., Roux, Ph., Gaudillière, N., Dirrenberger, J. & Morel, Ph. 2016. Large-scale 3D printing of ultra-high performance concrete – a new processing route for architects and builders. Materials and Design, 100: 2016. Pp. 102–109.

Hwang, D. & Khoshnevis, B. 2004. Concrete wall fabrication by contour crafting. 21st International Symposium on Automation and Robotics in Construction. Pp. 1–7.

Kashani, A. & Ngo, T. D. 2018. Optimisation of mixture properties for 3D printing of geopolymer concrete. 35th International Symposium on Automation and Robotics in Construction (ISARC 2018). Pp. 1–8.

Kazemian, A., Yuan, X., Cochran, E. & Khoshnevis, B. 2017a. Cementitious materials for construction-scale 3D printing: Laboratory testing of fresh printing mixture. Construction and Building Materials, 145: 2017. Pp. 639–647.

Kazemian, A., Yuan, X., Meier, R., Cochran, E. & Khoshnevis, B. 2017b. Construction-scale 3D printing: shape stability of fresh printing concrete. 12th International Manufacturing Science and Engineering Conference (MSEC2017). Pp. 1–5.

Kim, J. S., Kwon, S. H., Jang, K. P. & Choi, M. S. 2018. Concrete pumping prediction considering different measurement of the rheological properties. Construction and Building Materials, 171: 2018. Pp. 493–503.

Kolezynski, A., Krol, M. & Zychowicz. 2018. The structure of geopolymers–Theoretical studies. Journal of Molecular Structure, 1163: 2018. Pp. 465–471.

Kosmatka, S. H., Kerkhoff, B. & Panarese, W. C. 2002. Design and Control of Concrete Mixtures, EB001, 14th edition. Portland Cement Association, Skokie, Illinois, USA. 358 pages.

Krimi, I., Lafhaj, Z. & Ducoulombier, L. 2017. Prospective study on the integration of additive manufacturing to building industry–Case of a French construction company. Additive Manufacturing, 16: 2017. Pp. 107–114.

Labonnote, N., Rønnquist, A., Manum, B. & Rüther, P. 2016. Additive construction: State-of-the-art, challenges and opportunities. Automation in Construction, 72: 3. Pp. 347–366.

Lampinen, S. & Alonen, A. 2017. Lisäävän valmistuksen käyttö rakennusalalla. Tilannekatsaus 2017. 1st edition. Kevama Oy, Kuopio, Finland. 98 pages.

Lao, W., Li, M., Masia, L. & Tan, M. J. 2017. Approaching Rectangular Extrudate in 3D Printing for Building and Construction by Experimental Iteration of Nozzle Design. Solid Freeform Fabrication 2017: Proceedings of the 28th Annual International Solid Freeform Fabrication Symposium – An Additive Manufacturing Conference. Pp. 2612–2623.

Lao, W., Tay, D. Y. W., Quirin, D. & Tan, M. J. 2018. The effect of nozzle shapes on the compactness and strength of structures printed by additive manufacturing of concrete. Proceedings of the 3rd International Conference on Progress in Additive Manufacturing, (Pro-AM 2018). Pp. 80–86.

Leal da Silva, W. R. 2017. 3D Concrete Printing - Technological issues in concrete mix design and extrusion. [Presentation Slides]. [Referred 30.10.2018]. Available: https://www.dti.dk/projects/3d-printed-buildings/36993

Le, T. T., Austin, S. A., Lim, S., Buswell, R. A., Law, R., Gibb, A. G. F. & Thorpe, T. 2012a. Hardened properties of high-performance printing concrete. Cement and Concrete Research, 42: 3. Pp. 558–566.

Le, T. T., Austin, S. A., Lim, S., Buswell, R. A., Law, R., Gibb, A. G. F. & Thorpe, T. 2012b. Mix design and fresh properties for high-performance printing concrete. Materials and Structures, 45: 2012. Pp. 1221–1232.

Lim, J. H., Panda, B. & Pham, Q-C. 2018. Improving flexural characteristics of 3D printed geopolymer composites with in-process steel cable reinforcement. Construction and Building Materials, 178: 2018. Pp. 32–41.

Lloret, E., Shahab, A. R., Linus, M., Flatt, R. J., Gramazio, F., Kohler, M. & Langenberg, S. 2015. Complex concrete structures. Merging existing casting techniques with digital fabrication. Computer-Aided Design, 60: 2015. Pp. 40–49.

Ma, C-K., Awang, A. Z. & Omar, W. 2018a. Structural and material performance of geopolymer concrete: A review. Construction and Building Materials, 186: 2018. Pp. 90–102.

Ma, G., Li, Z., Wang, L. & Bai, G. 2019. Micro-cable reinforced geopolymer composite for extrusion-based 3D printing. Materials Letters, 235: 2019. Pp. 144–147.

Ma, G., Wang, L. & Ju, Y. 2018b. State-of-the-art of 3D printing technology of cementitious material—An emerging technique for construction. Science China Technological Sciences, 61: 4. Pp. 475–495.

M-tec. 2018. Duo-mix. [m-tec webpage]. [Referred 31.10.2018]. Available: https://m-tec.com/duo-mix/#fb0=3

M-tec. 2019. D20. [m-tec webpage]. [Referred 25.3.2019]. Available: https://m-tec.com/construction-site-equipment/machines/mixer/d20/

Nematollahi, B., Xia, M., Sanjayan, J. & Vijay, P. 2018. Effect of Type of Fiber on Inter-Layer Bond and Flexural Strengths of Extrusion-Based 3D Printed Geopolymer. Proceedings of the 2nd International Conference on Advanced Manufacturing and Materials (ICAMM 2018), Tokio, Japan, June 11–13 2018. Pp. 1–8.

Panda, B., Mohamed, N. A. N., Tay, D. Y. W., He, L. & Tan, M. J. 2018a. Effects of slag addition on bond strength of 3D printed geopolymer mortar: an experimental investigation. Proceedings of the 3rd International Conference on Progress in Additive Manufacturing (Pro-AM 2018). Pp. 62–67.

Panda, B., Paul, S. C. & Tan, M. J. 2017a. Anisotropic mechanical performance of 3D printed fiber reinforced sustainable construction material. Materials Letters, 209: 2017. Pp. 146–149.

Panda, B., Paul, S. C., Hui, L. J., Tay, Y. W. D. & Tan, M. J. 2017b. Additive manufacturing of geopolymer for sustainable built environment. Journal of Cleaner Production, 167: 2017. Pp. 281–288.

Panda, B., Paul, S. C., Mohamed, N. A. N., Tay, Y. W. D. & Tan, M. J. 2018b. Measurement of tensile bond strength of 3D printed geopolymer mortar. Measurement, 113: 2018. Pp. 108–116.

Panda, B. & Tan, M. J. 2018. Experimental study on mix proportion and fresh properties of fly ash based geopolymer for 3D concrete printing. Ceramics International, 44: 9. Pp. 10258–10265.

Paul, S. C., Tay, Y. W. D., Panda, B. & Tan, M. J. 2018a. Fresh and hardened properties of 3D printable cementitious materials for building and construction. Archives of Civil and Mechanical Engineering, 18: 1. Pp. 311–319.

Paul, S. C., van Zijl, G. P. A. G., Tan, M. J. & Gibson, I. 2018b. A review of 3D concrete printing systems and materials properties: current status and future research prospects. Rapid Prototyping Journal, 24: 4. Pp. 784–798.

PCI. 2019. Precast/ Prestressed Concrete Institute. Walls Precast Concrete. [PCI webpage]. [Referred 21.3.2019]. Available: https://www.pci.org/PCI/Resources/About_Precast/Walls/PCI/Design_Resources/About_Precast/Walls.aspx

PCM. 2019. PCM EcoMoineau™ MVA - MVA FF sludge pumps. [PCM webpage]. [Referred 22.3.2019]. Available: https://www.pcm.eu/en/industry/pcm-solutions/progressing-cavity-pumps/pcm-ecomoineau-mva-mva-ff-sludge-pumps

Pump. 2011. [web document]. [Referred 15.2.2019]. Available in PDF-file: https://resources.saylor.org/wwwresources/archived/site/wp-content/uploads/2011/04/Pump.pdf

Putzmeister. 2019. Buffer storages jt 5000. [Putzmeister webpage]. [Referred 22.3.2019]. Available: https://www.putzmeister.com/web/americas/products/-/product-category/series/4743956/4743966/5575740/concrete/buffer-storage/jt-5000/jt-5000

Renca. 2018. Fully-automatic mobile mixing plant for geopolymer and ordinary Portland cement concrete. [web document]. [Referred 30.10.2018]. Available in PDF-file: https://yadi.sk/i/983a8rSM3RQUaB

Riding, K. A., Vosahlik, J., Feys, D., Malone, T. & Lindquist, W. 2016. Best Practices for Concrete Pumping. Kansas Department of Transportation. [web document]. [Referred 8.11.2018]. Available in PDF-file: https://rosap.ntl.bts.gov/view/dot/31647/dot_31647_DS1.pdf?

Sanjayan, J. G., Nematollahi, B., Xia, M. & Marchment, T. 2018. Effect of surface moisture on inter-layer strength of 3D printed concrete. Construction and Building Materials, 172: 2018. Pp. 468–475.

Scutti. 2019. Ø 3500 SP SERIE. [Scutti webpage]. [Referred 22.3.2019]. Available: http://www.scuttinicola.com/steel_silos/bolted_silos/paneled_steel_silos_3500_sp.asp

SFS-EN ISO/ ASTM 52900. 2017. Additive manufacturing. General principles. Terminology. Helsinki: Finnish Standards Association. 13 p.

SFS-EN 1015-3. 1999. Methods of test for mortar for masonry. Part 3: Determination of consistence of fresh mortar (by flow table). Helsinki: Finnish Standards Association. 10 p.

SFS-EN 12390-1. 2012. Testing hardened concrete. Part 1: shape, dimensions and other requirements for specimens and moulds. Helsinki: Finnish Standards Association. 13 p.

SFS-EN 12390-3. 2009. Testing hardened concrete. Part 3: Compressive strength of test specimens. Helsinki: Finnish Standards Association. 19 p.

SFS-EN 12390-5. 2009. Testing hardened concrete. Part 5: Flexural strength of test specimens. Helsinki: Finnish Standards Association. 11 p.

SFS-EN 12390-6. 2009. Testing hardened concrete. Part 6: Tensile splitting strength of test specimens. Helsinki: Finnish Standards Association. 11 p.

SFS-EN 14488-4. 2008. Testing sprayed concrete. Part 4: Bond strength of cores by direct tension. Helsinki: Finnish Standards Association. 7 p.

SFS-EN 196-1. 2016. Methods of testing cement. Part 1: Determination of strength. Helsinki: Finnish Standards Association. 32 p

SFS-EN 196-3. 2016. Methods of testing cement. Part 3: Determination of setting times and soundness. Helsinki: Finnish Standards Association. 45 p.

Snyder. 2019. Cone bottom tanks. [Snyder Industries webpage]. [Referred 25.3.2019]. Available: http://www.snydernet.com/products/industrial-tanks/cone-bottom-tanks

Totalkustom. 2015. World's First 3D Printed Hotel in the Philippines, by Andrey Rudenko. Completed in 2015. [Totalkustom webpage]. [Referred 29.10.2018]. Available: http://www.totalkustom.com/3d-printed-hotel-suite.html

Verderflex. 2019. Rapide R6. [Verderflex webpage]. [Referred 25.3.2019]. Available: https://www.verderflex.com/en/peristaltic-industrial-tube-pumps/verderflex-rapide/r6/

Wolfs, R. J. M., Bos, F. P. & Salet, T. A. M. 2018. Early age mechanical behavior of 3D printed concrete: Numerical modelling and experimental testing. Cement and Concrete Research, 106: 2018. Pp. 103–116.

Yang, H., Chung, J. K. H., Chen, Y. & Li, Y. 2018. The cost calculation method of construction 3D printing aligned with internet of things. EURASIP Journal on Wireless Communications and Networking, 147: 2018. Pp. 1–9.

Zareiyan, B. & Khoshnevis, B. 2017. Effects of interlocking on interlayer adhesion and strength of structures in 3D printing of concrete. Automation in Construction, 83: 2017. Pp. 212–221.

Zhang, D. –W., Wang, D. –m., Lin, X. –Q. & Zhang, T. 2018. The study of the structure rebuilding and yield stress of 3D printing geopolymer pastes. Construction and Building Materials, 184: 2018. Pp. 575–580.

1. Mixability
    0. No uniform mixing, separates to clumps. Liquid does not absorb to dry materials.
    1. Mixing possible only partly. Clump formation and some unmixed material left.
    2. All ingredients are mixed but mixed material starts to break down in crumbles straight after.
    3. All ingredients are mixed together but all liquid does not absorb to ingredient and segregates.
    4. All ingredients mix well, some stiffness or low viscosity or segregation.
    5. All ingredients mix well, no clumps or unmixed material left, no segregation.
2. Initial state of mixed geopolymer
    0. Slurry state, cannot be handled with anything. Does not stick to itself when shaping, turns into crumples.
    1. Sticky and not shapeable or possible to shape but fractures partly.
    2. Possible to shape does not keep shape or does not fracture.
    3. Sticky and low slump, keeps shape partly.
    4. Keeps shape but partly sticky or low slump.
    5. Moldable, shapeable and keeps it shape.
3. Initial workable time
    0. Material sets right after mixing or not possible to shape material after 10 minutes.
    1. Material sets under minute or is not possible to shape after that time.
    2. Material sets under 2 minutes or is not possible to shape after that time.
    3. Material sets under 3 minutes or is not possible to shape after that time.
    4. Material sets under 4 minutes or is not possible to shape after that time.
    5. Material sets takes more than 5 minutes and shaping possible after that time.
4. Extrudability
    0. Material cannot be extruded at all.
    1. Part of material is set before all can be extruded.
    2. Tearing while extruding or inconsistent material flow.
    3. Material is start to tear after half way through of initial setting time
    4. Material is extrudable around 90% of initial setting time
    5. Material can be extruded through the initial setting time

5. Appearance after 1 day of curing
    0. Heavy calcium powder formation on top or breakable in hands.
    1. Does not break immediately, but still brittle. Powder formation.
    2. Some cracking on surfaces and noticeable powder formation
    3. Slight powder formation, some irregularity on surfaces.
    4. Some different colored spots and possible hair cracking.
    5. Uniform color, no powder formation and does not break in hands.
6. Water to silicate ratio
    0. Above 5.
    1. Above 4 to 5
    2. Above 3 to 4
    3. Above 2 to 3.
    4. Above 1 to 2.
    5. Under 1.
7. Silicate to binder ratio
    0. Over 4 or under 1.
    1. Between 3,5 to 4.
    2. Between 3 to 3,5
    3. Between 2,5 to 3 or between 1 to 1,5.
    4. Between 2,0 to 2,5.
    5. Between 1,5 to 2,0.
8. Al to Si ratio
    0. Over 3,1 or under 1.
    1. Between 1 to 1,2 or between 2,9 to 3,1.
    2. Between 1,2 to 1,4 or between 2,7 to 2,9
    3. Between 1,4 to 1,6 or between 2,5 to 2,7.
    4. Between 1,6 to 1,8 or between 2,3 to 2,5.
    5. Between 1,8 to 2,3
9. Waste materials
    0. Under 40%.
    1. 40 to 45%.
    2. 45 to 50%.
    3. 50 to 55%.
    4. 55 to 60%.
    5. 60% or higher.

APPENDIX II

Mix	1.	2.	3.	4.	5.	6.	7.	8.	9.	Total
3l*	4	4	5	7,5	5	7,5	5	4	4	46
3m*	3	3	5	7,5	5	7,5	3	5	5	44
3n	5	4	5	7,5	5	7,5	3	3	4	44
1q	4	4	5	7,5	5	7,5	3	4	4	44
4e	5	4	5	7,5	5	6	4	3	4	43,5
2m*	2	3	5	6	5	7,5	5	5	5	43,5
2l*	3	4	5	7,5	5	7,5	3	4	4	43
2n	5	3	5	7,5	5	7,5	3	3	4	43
3i	4	4	5	7,5	5	6	4	3	4	42,5
1l*	3	4	5	7,5	5	6	4	4	4	42,5
3f	4	4	4	6	5	6	4	3	4	40
5p	5	3	5	7,5	5	7,5	0	3	4	40
1n	2	4	5	4,5	5	7,5	3	3	4	38
3e	4	3	4	4,5	4	6	4	3	4	36,5
1e	3	4	5	6	2	6	4	3	3	36
2e	3	3	5	6	3	6	4	3	3	36
4p	3	3	5	6	5	7,5	0	3	3	35,5
1m*	2	4	2	1,5	5	7,5	5	3	4	34
1j	2	4	5	0	5	6	4	3	4	33
4n	2	2	5	1,5	5	7,5	3	3	4	33
2o	3	4	1	1,5	4	7,5	4	3	4	32
7c	3	3	4	4,5	3	6	4	1	2	30,5
2f	3	2	2	1,5	2	6	4	5	5	30,5
3g	4	3	5	7,5	4	0	0	3	4	30,5
2g	3	3	5	7,5	4	0	0	3	4	29,5
1h	4	4	5	7,5	1	0	0	5	3	29,5
6c	3	3	4	4,5	3	4,5	1	4	2	29
1d	3	3	3	3	2	6	1	5	3	29
1b	4	1	1	1,5	2	7,5	5	2	4	28
1o	2	1	1	0	4	7,5	5	3	4	27,5
3p	2	1	5	0	5	7,5	0	2	4	26,5
1f	1	1	1	1,5	1	6	4	5	5	25,5
2k	3	2	2	0	0	4,5	3	5	5	24,5
1k	3	2	2	0	0	6	1	5	5	24
2b	3	1	1	1,5	1	6	3	4	3	23,5
2p	1	1	5	0	5	7,5	0	0	4	23,5
3b	1	1	1	0	1	6	3	5	5	23
5c	3	2	0	0	2	6	3	4	3	23
2c	1	2	4	4,5	2	4,5	1	0	3	22
4c	2	2	0	0	2	6	1	5	3	21
1c	2	1	0	0	1	6	2	5	3	20
1i	2	4	5	0	2	0	0	5	2	20
2i	2	4	5	0	2	0	0	5	2	20
3k	3	2	2	0	0	6	1	4	2	20
4k	3	2	2	0	0	4,5	0	5	3	19,5
3c	1	1	3	0	0	6	1	2	5	19
1g	1	1	0	0	1	4,5	3	3	5	18,5
1a	0	0	0	0	0	6	1	5	4	16
1p	0	0	0	0	0	7,5	3	0	5	15,5